Statistical analysis

Age, height, body weight, body mass index (BMI), and osteoarthritis parameters (number of osteophytes, endoplate sclerosis, and disc narrowing) in the groups of subjects classified by the WISP1 SNP genotypes were compared by analysis of variance (ANOVA) and Kruskal–Wallis test. Stepwise regression analysis was carried out to assess the independent effect of four variables (age, height, body weight, WISP 1 SNP genotypes) on endplate sclerosis score. We also divided subjects into those having one or two allele(s) of the minor G allele (AG + GG) and those with only the major A allele (AA) encoded at the same locus. Multivariate logistic regression was used to estimate odds ratios and 95% confidence intervals (95% CIs) for these two groups and the risk of endplate sclerosis. Analyses for the association of WISP1 2364A/G genotypes and radiographic spinal endplate sclerosis were performed with adjustment for age. P values less than 0.05 were considered significant. Analysis was performed using StatView-J 4.5 software (SAS Institute, Cary, NC, USA).

Results

We analyzed the genotypes for the SNP of WISP1 gene at the 3′-UTR region (2364 A > G) in 304 subjects, using the TaqMan method. Among these postmenopausal Japanese women, 120 were AA homozygotes, 149 were AG heterozygotes, and 35 were GG homozygotes (Table 1). The allelic frequencies of this SNP in the present study were in Hardy–Weinberg equilibrium.

The background data (age, height, body weight, BMI) were not statistically different among these groups (Table 1). On ANOVA analysis, we found significant associations between WISP1 2364A/G genotype and endplate sclerosis score (Table 1; $P = 0.0062$). On Kruskal–Wallis analysis, we also found significant associations between WISP1 2364A/G genotype and endplate sclerosis score (Table 1; $P = 0.024$). Women with the AA allele had a significantly higher endplate sclerosis score than did subjects bearing at least one G allele (AG + GG). On the other hand, the occurrence of disc narrowing and osteophytes did not significantly differ among those SNP genotypes (see Table 1).

Recent studies have shown that the physical and constitutional factors contribute to spinal osteoarthritis. Therefore, we carried out stepwise regression analysis to assess the independent effect of age, height, body weight, and WISP1 SNP genotypes on endplate sclerosis score. Among these factors, only age and WISP1 SNP genotypes correlated significantly with spinal endplate sclerosis score (Table 2). The standard regression coefficients were 0.261 for age and −0.166 for WISP1 SNP genotypes.

Last, we analyzed the association between the alleic frequency of WISP1 SNP genotypes and endplate sclerosis score after stratification by age. In these analyses, we divided subjects into two groups, those who carried the G allele (GG or GA, $n = 184$) and with those who did not (AA, $n = 120$). We found that the subjects without the G allele (AA) were significantly overrepresented in the subjects having a one or more endplate sclerosis score compared in the subjects having no endplate sclerosis after being age-adjusted (Table 3; $P = 0.044$; odds ratio 1.78; 95% confidence interval 1.01–3.13 by logistic regression analysis). We also found that the subjects with the genotype AA were significantly

Table 1. Comparison of background and clinical characteristics among subjects with single nucleotide polymorphism (SNP) genotypes (AA genotype, AG genotype and GG genotype) in the WISP1 gene 3′-UTR region (2364A/G)

Items	Genotype (mean ± SD)			P value (ANOVA)	P value (Kruskal–Wallis)
	AA	AG	GG		
Number of subjects	120	149	35		
Age (years)	66.1 ± 9.2	66.3 ± 8.5	67.1 ± 10.6	NS	NS
Height (cm)	150.7 ± 5.6	150.2 ± 6.8	150.0 ± 5.0	NS	NS
Body weight (kg)	50.3 ± 7.6	50.2 ± 8.3	48.0 ± 5.4	NS	NS
BMI	22.1 ± 2.9	22.2 ± 2.9	21.3 ± 3.3	NS	NS
Endplate sclerosis	0.58 ± 1.09	0.34 ± 0.74	0.09 ± 0.28	0.0062	0.024
Osteophyte	5.89 ± 3.93	5.72 ± 3.40	5.57 ± 4.08	NS	NS
Disk narrowing	2.21 ± 1.79	2.09 ± 2.00	2.03 ± 1.86	NS	NS

BMI, body mass index; NS, not significant

Table 2. Results of stepwise regression analysis of four factors for endplate sclerosis score

Factors	F value			r.c.	s.r.c.
	Step 0	Step 1	Step 2	Step 2	($R^2 = 0.094$)
Intercept	63.7	12.8	9.4	−1.106	−1.106
WISP1 SNP genotypes (AA = 0, AG, GG = 1)			9.1	−0.297	−0.166
Age (years)		21.5	22.7	0.025	0.261
Weight (kg)			Not selected		
Height (cm)			Not selected		

r.c., regression coefficient; s.r.c., standard regression coefficient

Table 3. Association of WISP1 SNP genotype (2364A/G) in subjects with spinal endplate sclerosis after stratifying age

Group compared	AA vs. AG + GG		
	OR	*P* value	95% CI
Endplate sclerosis (≧1) (n = 235) versus no endplate sclerosis (=0) (n = 69)	1.78	0.044	1.01–3.13
Higher endplate sclerosis (≧2) (n = 271) versus lower endplate sclerosis (≦0) (n = 33)	2.91	0.0069	1.34–6.30

OR, odds ratio; 95% CI, 95% confidence interval

over-represented in the subjects having a higher (two or more) endplate sclerosis score compared in the subjects having lower (one or no) endplate sclerosis score after being age-adjusted (Table 3; P = 0.0069; odds ratio 2.91; 95% confidence interval 1.34–6.30 by logistic regression analysis). Thus, we suggest that a genetic variation at the WISP1 gene locus is associated with spinal osteoarthritis, especially with endplate sclerosis, independently with background parameters.

Discussion

The present study is the first report that shows the influence of a SNP of the WISP1 gene on spinal osteoarthritis. The WISP1 is an osteogenic potentiating factor promoting mesenchymal cell proliferation and osteoblastic differentiation while repressing chondrocytic differentiation [33]. We demonstrated that Japanese postmenopausal women who had the AA genotype at the WISP1 2364A/G SNP showed a significantly higher endplate sclerosis score of the spine. Our findings might also be supported by genetic linkage scan for early-onset osteoarthritis and chondrocalcinosis susceptibility loci that showed a linkage to chromosome 8q [36], which includes the WISP1 gene locus on 8q24.

It has been recently shown that haplotype analysis in LRP5 gene revealed that there was a common haplotype that provided a 1.6-fold-increased risk of knee osteoarthritis [37]. We have revealed that a SNP (Q89R) in the LRP5 gene is associated with spinal osteoarthritis [38]. It is also reported that there was a significant association of a functional genetic variant of secreted frizzled-related protein 3 (sFRP3), which antagonizes Wnt signaling, with hip osteoarthritis in women [39]. Taken together, our results and the recent evidence suggest that the Wnt-β-catenin signaling pathway including WISP1 is important in the pathogenesis of skeletal abnormality including osteoarthritis.

WISP1 is a member of the CCN family of connective tissue growth factors, which also includes WISP2 and WISP3. Members of the CCN family have been implicated in developmental processes such as chondrogenesis, osteogenesis, and angiogenesis [27–29]. Specifically, mutations of WISP3 cause the rare skeletal syndrome, progressive pseudorheumatoid dysplasia (PPD) [40]. In affected individuals, symptoms develop between the age of 3 years and 8 years and consist of stiffness and swelling of multiple joints, motor weakness, and joint contractures. It has been also reported that WISP3 polymorphisms were associated with susceptibility to juvenile idiopathic arthritis [41]. Moreover, the WISP3 was shown to be expressed in chondrocytes derived from human cartilage and be able to regulate type II collagen and aggrecan expression [42]. On the other hand, the expression of the WISP2 was preferentially detected in rheumatoid arthritis synovium [43]. These data suggest that CCN family members play a critical role in cartilage homeostasis. In the present study, we investigated a possible contribution of WISP1 polymorphism to spinal osteoarthritis in Japanese women. Taken together, the CCN family gene polymorphisms may affect the pathogenesis of cartilage disease.

In the present study, we excluded subjects with severe hip or knee arthritis, because these joint diseases themselves may induce spinal deformity or malalignment. Therefore, we could not assess such joint arthritis here. Recent studies have shown that some SNPs in the sFRP3 and LRP5 genes, involved in Wnt signaling, were associated with hip and knee osteoarthritis, respectively [37,39]. Moreover, WISP3 polymorphisms are associated with juvenile idiopathic arthritis that affects multiple joints [41]. In this regard, it may be important to examine the association of the SNPs in the WISP1 gene with hip and knee arthritis in the future. Meanwhile, it would be better if we had also evaluated the facet joint, because spinal osteoarthritis is represented not only by the anterior elements such as disc narrowing, osteophytosis, or endplate sclerosis but also by the posterior elements, especially a facet joint lesion. However, we here evaluated only the anterior elements of thoracolumbar vertebral bodies, because a reproducible semiquantitative assessment for facet joint using anteroposterior (A-P) and lateral X-ray radiographs has not been well established.

In conclusion, we have shown an association of the polymorphism in the WISP1 gene with a radiographic feauture of spinal endplate sclerosis in postmenopausal Japanese women. The women with AA genotypes had significantly higher endplate sclerosis scores. WISP1 genotyping may be benefical in the prevention and management of spinal osteoarthritis. Thus, the WISP1 would be a useful molecular target for the development of new diagnostic markers as well as therapeutic options in osteoarthritis.

Acknowledgments This work was partly supported by grants from the Japanese Ministry of Health, Labor, Welfare, Japan Society for the Promotion of Science, and the Ministry of Culture, Education, Sports, Science and Technology of Japan.

References

1. Creamer P, Hochberg MC (1997) Osteoarthritis. Lancet 350:503–508
2. Lane NE, Nevitt MC, Genant HK, Hochberg MC (1993) Reliability of new indices of radiographic osteoarthritis of the hand and hip and lumbar disc degeneration. J Rheumatol 20:1911–1918
3. O'Neill TW, McCloskey EV, Kanis JA, Bhalla AK, Reeve J, Reid DM, Todd C, Woolf AD, Silman AJ (1999) The distribution, determinants, and clinical correlates of vertebral osteophytosis: a population based survey. J Rheumatol 26:842–848
4. Spector TD, MacGregor AJ (2004) Risk factors for osteoarthritis: genetics. Osteoarthritis Cartilage 12:S39-S44
5. Loughlin J (2003) Genetics of osteoarthritis and potential for drug development. Curr Opin Pharmacol 3:295–299
6. Nusse R, Varmus HE (1992) Wnt genes. Cell 69:1073–1087
7. Rijsewijk F, Schuermann M, Wagenaar E, Parren P, Weigel D, Nusse R (1987) The *Drosophila* homolog of the mouse mammary oncogene int-1 is identical to the segment polarity gene wingless. Cell 50:649–657
8. Nusse R, Varmus HE (1982) Many tumors induced by the mouse mammary tumor virus contain a provirus integrated in the same region of the host genome. Cell 31:99–109
9. Barrow JR, Thomas KR, Boussadia-Zahui O, Moore R, Kemler R, Capecchi MR, McMahon AP (2003) Ectodermal Wnt3/beta-catenin signaling is required for the establishment and maintenance of the apical ectodermal ridge. Genes Dev 17:394–409
10. Soshnikova N, Zechner D, Huelsken J, Mishina Y, Behringer RR, Taketo MM, Crenshaw EB III, Birchmeier W (2003) Genetic interaction between Wnt/beta-catenin and BMP receptor signaling during formation of the AER and the dorsal-ventral axis in the limb. Genes Dev 17:1963–1968
11. Cadigan KM, Nusse R (1999) Wnt signaling: a common theme in animal development. Genes Dev 11:3286–3305
12. Bennett CN, Longo KA, Wright WS, Suva LJ, Lane TF, Hankenson KD, MacDougald OA (2005) Regulation of osteoblastogenesis and bone mass by Wnt10b. Proc Natl Acad Sci U S A 102:3324–3329
13. Bain G, Muller T, Wang X, Papkoff J (2003) Activated beta-catenin induces osteoblast differentiation of C3H10T1/2 cells and participates in BMP2 mediated signal transduction. Biochem Biophys Res Commun 301:84–91
14. Tamai K, Semenov M, Kato Y, Spokony R, Liu C, Katsuyama Y, Hess F, Saint-Jeannet JP, He X (2000) LDL-receptor-related proteins in Wnt signal transduction. Nature (Lond) 407:530–553
15. Mao J, Wang J, Liu B, Pan W, Farr GH III, Flynn C, Yuan H, Takada S, Kimelman D, Li L, Wu D (2001) Low-density lipoprotein receptor-related protein-5 binds to Axin and regulates the canonical Wnt signaling pathway. Mol Cell 7:801–809
16. Gong Y, Slee RB, Fukai N, Rawadi G, Roman-Roman S, et al. (2001) LDL receptor-related protein 5 (LRP5) affects bone accrual and eye development. Cell 107:513–523
17. Kato M, Patel MS, Levasseur R, Lobov I, Chang BH, Glass DA II, Hartmann C, Li L, Hwang TH, Brayton CF, Lang RA, Karsenty G, Chan L (2002) Cbfa1-independent decrease in osteoblast proliferation, osteopenia, and persistent embryonic eye vascularization in mice deficient in Lrp5, a Wnt coreceptor. J Cell Biol 157:303–314
18. Boyden LM, Mao J, Belsky J, Mitzner L, Farhi A, Mitnick MA, Wu D, Insogna K, Lifton RP (2002) High bone density due to a mutation in LDL-receptor-related protein 5. N Engl J Med 346:1513–1521
19. Little RD, Carulli JP, Del Mastro RG, Dupuis J, Osborne M, et al (2002) A mutation in the LDL receptor-related protein 5 gene results in the autosomal dominant high-bone-mass trait. Am J Hum Genet 70:11–19
20. Urano T, Shiraki M, Ezura Y, Fujita M, Sekine E, Hoshino S, Hosoi T, Orimo H, Emi M, Ouchi Y, Inoue S (2004) Association of a single-nucleotide polymorphism in low-density lipoprotein receptor-related protein 5 gene with bone mineral density. J Bone Miner Metab 22:341–345
21. Mizuguchi T, Furuta I, Watanabe Y, Tsukamoto K, Tomita H, Tsujihata M, Ohta T, Kishino T, Matsumoto N, Minakami H, Niikawa N, Yoshiura K (2004) LRP5, low-density-lipoprotein-receptor-related protein 5, is a determinant for bone mineral density. J Hum Genet 49:80–86
22. Ferrari SL, Deutsch S, Choudhury U, Chevalley T, Bonjour JP, Dermitzakis ET, Rizzoli R, Antonarakis SE (2004) Polymorphisms in the low-density lipoprotein receptor-related protein 5 (LRP5) gene are associated with variation in vertebral bone mass, vertebral bone size, and stature in whites. Am J Hum Genet 74:866–875
23. Lau HH, Ng MY, Ho AY, Luk KD, Kung AW (2005) Genetic and environmental determinants of bone mineral density in Chinese women. Bone (NY) 36:700–709
24. Sen M, Lauterbach K, El-Gabalawy H, Firestein GS, Corr M, Carson DA (2000) Expression and function of wingless and frizzled homologs in rheumatoid arthritis. Proc Natl Acad Sci USA 97:2791–2796
25. James IE, Kumar S, Barnes MR, Gress CJ, Hand AT, Dodds RA, Connor JR, Bradley BR, Campbell DA, Grabill SE, Williams K, Blake SM, Gowen M, Lark MW (2000) FrzB-2: a human secreted frizzled-related protein with a potential role in chondrocyte apoptosis. Osteoarthritis Cartilage 8:452–463
26. Ryu JH, Kim SJ, Kim SH, Oh CD, Hwang SG, Chun CH, Oh SH, Seong JK, Huh TL, Chun JS (2002) Regulation of the chondrocyte phenotype by beta-catenin. Development (Camb) 129:5541–5550
27. Bork P (1993) The modular architecture of a new family of growth regulators related to connective tissue growth factor. FEBS lett 327:125–130
28. Brigstock DR (1999) The connective tissue growth factor/cysteine-rich 61/nephroblastoma overexpressed (CCN) family. Endcr Rev 20:189–206
29. Perbal B (2001) NOV (nephroblastoma overexpressed) and the CCN family of genes: structural and functional issues. Mol Pathol 54:57–79
30. Pennica D, Swanson TA, Welsh JW, Roy MA, Lawrence DA, et al. (1998) WISP genes are members of the connective tissue growth factor family that are up-regulated in wnt-1-transformed cells and aberrantly expressed in human colon tumors. Proc Natl Acad Sci USA 95:14717–14722
31. Xu L, Corcoran RB, Welsh JW, Pennica D, Levine AJ (2000) WISP-1 is a Wnt-1- and beta-catenin-responsive oncogene. Genes Dev 14:585–595
32. Desnoyers L, Arnott D, Pennica D (2001) WISP-1 binds to decorin and biglycan. J Biol Chem 276:47599–47607
33. French DM, Kaul RJ, D'Souza AL, Crowley CW, Bao M, Frantz GD, Filvaroff EH, Desnoyers L (2004) WISP-1 is an osteoblastic regulator expressed during skeletal development and fracture repair. Am J Pathol 165:855–867
34. Yu W, Gluer CC, Fuerst T, Grampp S, Li J, Lu Y, Genant HK (1995) Influence of degenerative joint disease on spinal bone mineral measurements in postmenopausal women. Calcif Tissue Int 57:169–174
35. Asai T, Ohkubo T, Katsuya T, Higaki J, Fu Y, Fukuda M, Hozawa A, Matsubara M, Kitaoka H, Tsuji I, Araki T, Satoh H, Hisamichi S, Imai Y, Ogihara T (2001) Endothelin-1 gene variant associates with blood pressure in obese Japanese subjects: the Ohasama Study. Hypertension 38:1321–1324
36. Baldwin CT, Farrer LA, Adair R, Dharmavaram R, Jimenez S, Anderson L (1995) Linkage of early-onset osteoarthritis and chondrocalcinosis to human chromosome 8q. Am J Hum Genet 56: 692–697
37. Smith AJ, Gidley J, Sandy JR, Perry MJ, Elson CJ, Kirwan JR, Spector TD, Doherty M, Bidwell JL, Mansell JP (2005) Haplotypes of the low-density lipoprotein receptor-related protein 5 (LRP5) gene: are they a risk factor in osteoarthritis? Osteoarthritis Cartilage 13:608–613
38. Urano T, Shiraki M, Narusawa K, Usui T, Sasaki N, Hosoi T, Ouchi Y, Nakamura T, Inoue S. (2007) Q89R polymorphism in the LDL receptor-related protein 5 gene is associated with spinal osteoarthritis in postmenopausal Japanese women. Spine 32:25–29
39. Loughlin J, Dowling B, Chapman K, Marcelline L, Mustafa Z, Southam L, Ferreira A, Ciesielski C, Carson DA, Corr M (2004) Functional variants within the secreted frizzled-related protein 3 gene are associated with hip osteoarthritis in females. Proc Natl Acad Sci USA 101:9757–9762

40. Hurvitz JR, Suwairi WM, Van Hul W, El-Shanti H, Superti-Furga A, Roudier J, Holderbaum D, Pauli RM, Herd JK, Van Hul EV, Rezai-Delui H, Legius E, Le Merrer M, Al-Alami J, Bahabri SA, Warman ML (1999) Mutations in the CCN gene family member WISP3 cause progressive pseudorheumatoid dysplasia. Nat Genet 23:94–98
41. Lamb R, Thomson W, Ogilvie E, Donn R, British Society of Paediatric and Adolescent Rheumatology (2005) Wnt-1-inducible pathway protein 3 and susceptibility to juvenile idiopathic arthritis. Arthritis Rheum 52:3548–3553
42. Sen M, Cheng YH, Goldring MB, Lotz MK, Carson DA (2004) WISP3-dependent regulation of type II collagen and aggrecan production in chondrocytes. Arthritis Rheum 50:488–497
43. Tanaka I, Morikawa M, Okuse T, Shirakawa M, Imai K (2005) Expression and regulation of WISP2 in rheumatoid arthritic synovium. Biochem Biophys Res Commun 334:973–978

THE JOURNAL OF BIOLOGICAL CHEMISTRY VOL. 282, NO. 8, pp. 5736–5748, February 23, 2007

α-Synuclein Stimulates Differentiation of Osteosarcoma Cells

*RELEVANCE TO DOWN-REGULATION OF PROTEASOME ACTIVITY**

Received for publication, June 28, 2006, and in revised form, December 15, 2006 Published, JBC Papers in Press, December 22, 2006, DOI 10.1074/jbc.M606175200

Masayo Fujita[‡], Shuei Sugama[‡], Masaaki Nakai[‡], Takato Takenouchi[§], Jianshe Wei[‡], Tomohiko Urano[¶], Satoshi Inoue[¶], and Makoto Hashimoto[‡1]

From the [‡]Laboratory for Chemistry and Metabolism, Tokyo Metropolitan Institute for Neuroscience, Fuchu, Tokyo 183-8526, Japan, [§]Transgenic Animal Research Center, National Institute of Agrobiological Sciences, Tsukuba, Ibaraki 305-8634, Japan, and [¶]Department of Geriatrics and Gerontology, School of Medicine, University of Tokyo, Tokyo 113-8655, Japan

Because a limited study previously showed that α-synuclein (α-syn), the major pathogenic protein for Parkinson disease, was expressed in differentiating brain tumors as well as various peripheral cancers, the main objective of the present study was to determine whether α-syn might be involved in the regulation of tumor differentiation. For this purpose, α-syn and its non-amyloidogenic homologue β-syn were stably transfected to human osteosarcoma MG63 cell line. Compared with β-syn-overexpressing and vector-transfected cells, α-syn-overexpressing cells exhibited distinct features of differentiated osteoblastic phenotype, as shown by up-regulation of alkaline phosphatase and osteocalcin as well as inductive matrix mineralization. Further studies revealed that proteasome activity was significantly decreased in α-syn-overexpressing cells compared with other cell types, consistent with the fact that proteasome inhibitors stimulate differentiation of various osteoblastic cells. In α-syn-overexpressing cells, protein kinase C (PKC) activity was significantly decreased, and reactivation of PKC by phorbol ester significantly restored the proteasome activity and abrogated cellular differentiation. Moreover, activity of lysosome was up-regulated in α-syn-overexpressing cells, and treatment of these cells with autophagy-lysosomal inhibitors resulted in a decrease of proteasome activity associated with up-regulation of α-syn expression, leading to enhance cellular differentiation. Taken together, these results suggest that the stimulatory effect of α-syn on tumor differentiation may be attributed to down-regulation of proteasome, which is further modulated by alterations of various factors, such as protein kinase C signaling pathway and a autophagy-lysosomal degradation system. Thus, the mechanism of α-syn regulation of tumor differentiation and neuropathological effects of α-syn may considerably overlap with each other.

α-Synuclein (α-syn)[2] is a presynaptic protein that belongs to the syn family of peptides with two other members, β- and γ-syn (1, 2). These proteins are characterized by a native unfolded structure with a highly conserved N-terminal region and a divergent C-terminal acidic region (3). However, the most striking feature is that α-syn possesses a highly hydrophobic domain in the middle region that was previously purified from Alzheimer disease brain amyloid (4). Due to this hydrophobic domain, α-syn forms toxic protofibrils that might cause synaptic injury and dysfunction (5). The importance of α-syn in the pathogenesis of neurodegenerative disorders was further augmented by identification of missense mutations of α-syn in familial Parkinson disease (PD) (6–8). Subsequently, numerous histological studies have shown that α-syn is a major constituent in Lewy bodies and dystrophic neuritis in sporadic PD and diffuse Lewy body disease (2). Immunoreactivity of α-syn was also shown in glial cell inclusions in multiple system atrophy (2). By contrast, β-syn, which lacks the majority of the hydrophobic domain in the middle region, was protective against protofibrils of α-syn (9, 10). Thus, these results support the contention that α- and β-syn may play a central role in the pathogenesis of neurodegenerative diseases.

On the other hand, γ-syn, the less conserved third member of the syn family of peptides, was identified as a breast cancer-specific gene product (11) and has been extensively studied in a variety of cancers, such as breast cancer, ovarian cancer, liver cancer, pancreatic adenocarcinoma, and bladder cancer (11–15). Because expression levels of γ-syn were well correlated with the presence of metastatic lesions, it has been generally thought that γ-syn might regulate tumor invasiveness and metastasis (16, 17). Several studies indicated that γ-syn might be involved in the deregulation of cell cycle in cancer. For example, γ-syn interacted with a mitotic spindle checkpoint protein, BubR1, leading to decreased checkpoint function and tumor progression (18, 19). Moreover, γ-syn stimulated cell proliferation by augmenting estrogen receptor-mediated signaling in breast cancer cells (20). Thus, the role of γ-syn has been investigated mainly in the area of tumor biology.

* This work was supported in part by a grant-in-aid for Science Research from the Ministry of Education, Culture, Sports, Science, and Technology, Japan and a project grant from Tokyo Metropolitan Organization. The costs of publication of this article were defrayed in part by the payment of page charges. This article must therefore be hereby marked "*advertisement*" in accordance with 18 U.S.C. Section 1734 solely to indicate this fact.

[1] To whom correspondence should be addressed: Laboratory for Chemistry and Metabolism, Tokyo Metropolitan Institute for Neuroscience, 2–6 Musashidai, Fuchu, Tokyo 183-8526, Japan. Tel.: 81-42-325-3881; Fax: 81-42-321-8678; E-mail address: mhashimoto@tmin.ac.jp.

[2] The abbreviations used are: syn, synuclein; PD, Parkinson disease; UPS, ubiquitin-proteasome system; PKC, protein kinase C; PMA, 12-myristate 13-acetate; 4αPDD, 4α-phorbol 12,13-didecanoate; 3-MA, 3-methyladenine; Rb, retinoblastoma; RT, reverse transcriptase; CAPS, 3-(cyclohexylamino)-1-propanesulfonic acid; LSCM, laser-scanning confocal microscope; ALP, alkaline phosphatase; PBS, phosphate-buffered saline; LSCM, laser-scanning confocal microscope.

A recent study, however, suggests that molecular pathways shared by neurodegenerative disease and cancer may be considerably overlapped than thought before. Supporting this notion, it has been recently shown that several familial PD-causing factors are involved in the pathogenesis of cancer (21). First, overexpression of the PARK2 parkin, which functions as an E3 ligase in the ubiquitin-proteasome system (UPS), resulted in growth suppression in hepatocellular carcinoma cells (22). Furthermore, ectopic expression of parkin reportedly reduced *in vivo* tumorigenesis in nude mice (23). Second, the PARK5 ubiquitin C-terminal hydrolase light chain-1, which acts as a de-ubiquitinating enzyme in UPS, was shown to suppress proliferation of a lung cancer cells (24). Other evidence suggests that ubiquitin C-terminal hydrolase light chain-1 might be involved in the degradation of p27, a cyclin-dependent kinase inhibitor (25). Third, the PARK7 DJ-1 was first identified as an oncogene product that stimulated transformation of NIH3T3 cells in coordination with Ras (26). DJ-1 was recently shown to up-regulate the phosphatidylinositol 3-kinase pathway through inhibition of the tumor suppressor phosphatase PTEN, leading to enhance survival of cancer (27).

In the same context one may wonder if α- and β-syn, the central players in the pathogenesis of PD, might play some important roles for the regulation of cancer. Indeed, α-syn was widely expressed in a variety of brain tumors, such as medulloblastoma, neuroblastoma, pineoblastoma, and ganglioma (28, 29). Furthermore, both α- and β-syn were shown to be expressed in the peripheral cancers, including ovarian and breast cancers (30). Although the role of syn proteins in the pathogenesis of cancer is unclear, a limited number of studies suggest that α-syn might be involved in the regulation of tumor differentiation. Supporting this possibility, α-syn was preferentially expressed in brain tumors showing neuronal differentiation (28). In cell cultures expression of α-syn was increased during the hematopoietic differentiation of K562 myelogenous leukemia cells (31). Similarly, it was shown that α-syn was up-regulated during neural differentiation of pheochromocytoma PC12 cells (32). Thus, distinct from the possible role of γ-syn for tumor metastasis, α-syn might be involved in tumor differentiation.

Accordingly, the main objective of the present study was to determine whether α- and/or β-syn might regulate growth and differentiation of cancer cells. For this purpose, α- and β-syn were stably overexpressed in MG63 human osteosarcoma cells. We found that compared with vector-transfected and β-syn-overexpressing cells, α-syn-overexpressing cells exhibited distinct phenotype of differentiated osteoblastic cells. Mechanistically, α-syn may cause down-regulation of proteasome activity, leading to accelerate cellular differentiation. Further studies revealed that down-regulation of proteasome activity by α-syn was regulated by alteration of various factors, including PKC signaling activities and the autophagy-lysosomal pathway in α-syn-overexpressing cells.

EXPERIMENTAL PROCEDURES

Reagent—Chemical reagents include MG132 and lactacystin (purchased from EMD Biosciences, San Diego, CA), rotenone, 12-myristate 13-acetate (PMA), 4α-phorbol 12,13-didecanoate (4αPDD), leupeptin, chelerythrine chloride, and 3-methyladenine (3-MA) (obtained from Sigma), and caspase I inhibitor and III inhibitors (Ac-AAVALLPAVLLALLAP-YVAD-CHO, Ac-AAVALLPAVLLALLAP-DEVD-CHO) (Calbiochem) were applied to cell cultures at indicated concentrations.

Antibodies used are as follows. Monoclonal antibodies, anti-α-syn (syn-1), anti-β-syn, anti-PKCε, and anti-retinoblastoma (Rb) were purchased from BD Biosciences. Monoclonal anti-β-actin (AC-15) was obtained from Sigma. Monoclonal antibodies anti-p21 and anti-cyclin B1, rabbit polyclonal antibodies anti-p15, anti-cyclin D1, anti-cyclin-dependent kinase 4, and anti-phosphorylated Rb, and goat polyclonal anti-osteocalcin antibody were from Santa Cruz Biotechnology (Santa Cruz, CA). Monoclonal anti-ubiquitin antibody was from Chemicon (Temecula, CA). Monoclonal anti-19 S proteasome S6a subunit antibody was from Biomol (Plymouth Meeting, PA). Rabbit polyclonal anti-cathepsin B was from Calbiochem. Rabbit polyclonal antibodies, anti-C-terminal α-syn, and anti-β-syn were previously described (33, 34). Alexa fluor 488-conjugated anti-goat secondary antibody, Alexa fluor 488-conjugated anti-rabbit secondary antibody, and Alexa fluor 555-conjugated anti-mouse secondary antibody were from Invitrogen.

Cell Cultures and Transfection—MG63 and 293T cells were both cultured in Dulbecco's modified Eagle's medium (high glucose) containing 10% fetal calf serum (BioWest, Nuaille, France) and 1% v/v penicillin/streptomycin (Invitrogen) in a 5% CO_2, 95% air atmosphere. MG63 cells exhibited both α- and β-syn transcripts by RT-PCR analysis, but their protein expressions were hardly detectable by immunoblot analysis (data not shown). For stable transfection, MG63 cells were transfected with pCEP4 expression vector (Invitrogen) or pCEP4 containing either human α- or β-syn cDNA (34) using Lipofectamine 2000 (Invitrogen). After 2~3 weeks of incubation in the presence of 200 μg/ml hygromycin B (EMD Biosciences), the resistant colonies of cells (~20) were isolated. These stable cell lines were routinely maintained in the presence of 50 μg/ml hygromycin B. 293T cells were transiently transfected with p-Target expression vector (Promega, Madison, WI) containing human p21 cDNA insert.[3]

Reverse Transcriptase (RT)-PCR—Total RNA was isolated from cultured cells using the RNA extraction buffer ISOGEN (Nippon Gene, Tokyo, Japan). cDNA was synthesized from 2 μg of total RNA using the Superscript III First-Strand Synthesis system (Invitrogen) according to the manufacturer's instruction.

PCR amplification was carried out using Taq PCR polymerase (ABgene, Tokyo, Japan), and the amplified products were resolved by agarose gel electrophoresis. The following primers were used for PCR. Human α-syn (NM_000345): sense, 5′-ATGGATGTATTCATGAAAGGACTTTC-3′ (47–72-oligonucleotide position), antisense, 5′-GGCTTCAGGTTCGTAGTCTTGATAC-3′ (the 442–466 oligonucleotide position); human β-syn (BT006627): sense, 5′-ATGGACGTGTTCATGAAGGGC-3′ (1–21-oligonucleotide position), antisense, 5′-CTACGCCTCTGGCTCATACTC-3′ (385–405-oligonucleotide position); human cyclophilin A (NM_021130): sense, 5′-TACTATTAG-

[3] T. Urano, unpublished information.

CCATGGTCAAC-3′ (62–81-oligonucleotide position), antisense 5′-GTCTTGCCATTCCTGGACCC-3′ (508–527-oligonucleotide position); human liver/bone/kidney-type alkaline phosphatase (ALP) (AB011406): sense, 5′-GGGGGTGGCCGGAAATACAT-3′ (834–853-oligonucleotide position), antisense, 5′-GGGGGCCAGACCAAAGATAG-3′ (1357–1376-oligonucleotide position); human osteocalcin (X51699): sense, 5′-ATGAGAGCCCTCACACTCCTC-3′ (19–39-oligonucleotide position), antisense, 5′-GCCGTAGAAGCGCCGATAGGC-3′ (292–312-oligonucleotide position).

Immunoblot and Co-immunoprecipitation Analyses—Immunoblot analysis was performed as previously described (34). Briefly, cells were harvested and dissolved in lysis buffer (1% Nonidet P-40, 50 mM HEPES, 150 mM NaCl, 10% glycerol, 1.5 mM $MgCl_2$, 1 mM EGTA, 100 mM sodium fluoride, and protease inhibitor mixture (Nakarai Tesque, Kyoto, Japan)). Protein concentrations of the cell lysates were determined Bio-Rad protein assay reagent. Cell extracts (10 μg) were then resolved by SDS-PAGE (10 or 16%) and electroblotted onto nitrocellulose membranes (GE Healthcare) with CAPS buffer (pH 11.0). The membranes were blocked with 3% bovine serum albumin (BSA) in Tris-buffered saline (TBS: 25 mM Tris-HCl (pH 7.5), 150 mM NaCl) plus 0.2% Tween 20 followed by an incubation with primary antibodies in TBS containing 3% BSA. After washing, the membranes were further incubated with second antibody conjugated with horseradish peroxidase (GE Healthcare) in Tris-buffered saline (1:10,000). Finally, the target proteins were visualized with the ECL plus system (GE Healthcare). The intensity of the band was measured using BioMax 1D image analysis soft ware (Eastman Kodak Co.). In some experiments 293T cells were transfected with p-Target vector (Promega) with or without human p21 cDNA insert, and cell extracts were used for controls. Recombinant human α- and β-syn were also used for positive controls (9).

Immunoprecipitation was performed as previously described (35). Briefly, cell extracts (200 μg) were preabsorbed with protein G-Sepharose (GE Healthcare) for 1 h, and the precleared lysates were incubated with either syn-1 or mouse IgG control (each 1 μg) overnight at 4 °C followed by incubation with protein G-Sepharose. The immune complexes were then washed three times with the lysis buffer. The samples were then heated in the SDS sample buffer for 5 min and subjected to immunoblotting.

Immunofluorescence Study—Cells were seeded onto poly-L-lysine-coated glass coverslips, grown to 70% confluence, fixed in 4% paraformaldehyde for 30 min and pretreated with 0.1% Triton X-100 in phosphate-buffered saline (PBS) for 20 min. Fixed cells were blocked with PBS containing 3% goat serum and 5% bovine serum albumin at room temperature. For staining, cells were incubated overnight at 4 °C with primary antibody (or antibodies for double staining). After washing, cells were incubated with Alexa fluor-conjugated secondary antibody (or antibodies for double staining) (Invitrogen) for 1 h at room temperature. Control experiments included immunostaining in the absence of primary antibody. Coverslips were air-dried, mounted on slides with Gel/Mount (Biomeda Corp., Foster City, CA), and imaged with the laser-scanning confocal microscope (LSCM) (Olympus, FV1000, Tokyo, Japan).

Cell Cycle Analysis Using Flow Cytometry—Cells seeded at 1×10^5 cells in 6-well cell culture plates were incubated under low serum (0.1%) conditions for 24 h, treated with 10% serum for 6, 12, 18, 24, and 96 h, and harvested using trypsin-EDTA. After washing with PBS, cells were fixed by ice-cold ethanol to final concentration of 70%. The cells were then resuspended in PBS containing 0.5 mg/ml RNaseA (Nakarai Tesque), incubated for 30 min at 37 °C, and followed by staining with propidium iodide (10 μg/ml) for 10 min at room temperature. Before flow cytometry analysis, the stained cells were filtrated with nylon mesh. The fluorescence signals of 2×10^4 cells were recorded by EPICS ALTRA (Beckman Coulter, Fullerton, CA). The distribution of cell cycle phase was analyzed by Multicycle software (Phoenix Flow Systems, San Diego, CA).

Measurement of ALP Activity—Cellular activities of ALP were determined as described previously with some modifications (36). Briefly, cells were grown until confluency under the 10% serum conditions in 6-well cell culture plates. Cells were then washed twice, harvested into PBS, and sonicated by ultrasonic disruptor (TOMY, Tokyo, Japan) for 20 s. After centrifugation of the cell preparations at 15,000 rpm for 10 min, the supernatants were recovered and assessed for protein concentration. The supernatants (10 μg) were then incubated in the ALP assay buffer containing 10 mM *p*-nitrophenyl phosphate (Sigma), 100 mM glycine, 1 mM $ZnCl_2$, and 1 mM $MgCl_2$ (pH 10.4). After 90 min of incubation at 37 °C, ALP activity was determined by monitoring the amount of released *p*-nitrophenol at 415 nm. Dissolved *p*-nitrophenol in assay buffer was used to establish the standard for quantification. The released *p*-nitrophenol was adjusted by the amount of protein and described as nmol/min/mg of protein.

Increased levels of the cellular ALP activities were further confirmed by direct stain of the cells. The cells reached confluency were fixed with 70% ethanol, washed twice with Tris-buffered saline, and incubated with nitro blue tetrazolium chloride/5-bromo-4-chloro-3-indolyl phosphate *p*-toluidine salt ALP substrate solution (Roche Applied Science) for 2 h. The visualized image was then photographed.

Mineralization Assay—Mineralization of MG63 cells was performed as previously described (36) with some modifications. Briefly, cells were grown until confluency under the 10% serum conditions in 24-well cell culture plates. The cells were further incubated in α-minimal essential medium (Invitrogen) plus 10% serum in the presence of 10 mM β-glycerophosphate (Sigma) and 50 μg/ml ascorbic acid with or without the addition of various chemical reagents. The media were regularly changed twice a week. After 4 weeks, cells were evaluated for the extent of matrix mineralization by either alizarin red staining or von Kossa staining. For alizarin red staining, the cells were fixed with 70% ethanol for 30 min at room temperature. Then the cells were incubated with 40 mM alizarin red-S (Sigma) for 10 min and washed 4 times with distilled water. The visualized image was photographed. For von Kossa staining, the cells were fixed with 10% neutralized formaldehyde for 30 min at room temperature. The fixed cells were incubated with 5% silver nitrate for 5 min under the exposure to the sunlight. The reaction was stopped by the addition of 5% sodium thiosulfate.

The stained cells were washed four times with distilled water and imaged with microscope.

Evaluation of Proteasome and Cathepsin B Activity—Measurement of proteasome and cathepsin B activity was done as previously described with modifications (37). Briefly, cells reaching confluency in 6-well cell culture plates were incubated under the low serum (0.1%) conditions for 24 h and treated with 10% serum with or without treatment of various reagents. After the indicated times (0, 6, or 12 h), the cells were harvested in buffer containing 50 mM HEPES (pH 7.4), 10 mM EDTA, and 10 mM NaCl, subjected to freezing and thawing to rapture cell membranous structures, and then centrifuged at 15,000 rpm for 10 min. For the measurement of proteasome activity, 10 μg of the supernatants were incubated in assay buffer containing 50 mM HEPES (pH 7.4), 10 mM EDTA, 10 mM NaCl, and 40 μM benzyloxycarbonyl-Leu-Leu-Glu-amidomethylcoumarin fluorogenic proteasome substrate (Chemicon). For cathepsin B activity, 10 μg of the supernatants were incubated in buffer containing 50 mM HEPES (pH 6.0), 10 mM EDTA, 10 mM NaCl, and 40 μM benzyloxycarbonyl-Arg-Arg-amidomethylcoumarin fluorogenic cathepsin B substrate (Chemicon). These enzyme activities were assayed by continuous recording of the fluorescence activity released from fluorogenic substrate using Berthold Mithras LB940 microplate reader (Berthold, Bad Wildbad, Germany) for 1 h at 37 °C (excitation, 380 nm; emission, 460 nm), and the reaction rate was analyzed. These enzyme activities were described as arbitrary unit/min/mg of protein.

Evaluation of PKC Activity—PKC activity was determined using PepTag nonradioactive PKC assay kit (Promega) according to the manufacture's instruction. Briefly, cells reaching confluency in 6-well cell culture plates were treated with or without PMA for 20 min and harvested in extraction buffer (25 mM Tris-HCl (pH 7.4), 0.5 mM EDTA, 0.5 mM EGTA, 10 mM β-mercaptoethanol, 100 mM phenylmethylsulfonyl fluoride, and protease inhibitor mixture (Nakarai Tesque)). Cell extracts were then sonicated by ultrasonic disruptor (TOMY) for 20 s and centrifuged at 15,000 rpm for 15 min. The supernatants were used for the assay. The reaction was performed at 30 °C for 30 min in assay solution including, PepTag C1 peptide (0.4 μg/μl) and 5 μg of protein sample. The samples were separated on the 0.8% agarose gel and visualized on a transilluminator. The intensity of fluorescence of the phosphorylated peptides were quantified using BioMax 1D image analysis soft ware (Kodak).

Electron Microscopy—Electron microscopy analysis was performed as previously described with minor modifications (38). Briefly, cells were harvested using trypsin-EDTA and fixed by 2.5% glutaraldehyde in 0.1 M sodium cacodylate buffer at 4 °C for 2 h. After centrifugation, cells were washed with 0.1 M sodium cacodylate buffer 3 times. Cell pellets were obtained by centrifuge, post-fixed in 1% osmium tetroxide and 1% potassium ferrocyanide at room temperature for 2 h, and processed for embedding in Quetol 812 (Nisshin EM, Tokyo, Japan). Ultrathin sections were stained with uranyl acetate and lead nitrate and observed by a Hitachi H-7500 electron microscope.

Statistical Analysis—All values in the figures are expressed as means ± S.D. To determine statistical significance, the values were compared by two group *t* tests. The differences were considered as significant if *p* values were less than 0.05.

RESULTS

Overexpression of Syn in MG63 Osteosarcoma Cells—To investigate the effect of syn on growth and differentiation of tumor cells, MG63 osteosarcoma cells were stably transfected with α- or β-syn cDNA. Three high expressors of α-syn (clones α1, α5, and α15) and β-syn (clones β5, β8, and β13) were selected on the basis of immunoblot analysis together with empty vector-transfected cells (clones v2, v5, and v10) (Fig. 1*A*). For the majority of experiments, clone α1, the high expresser of α-syn, and clones β5 and v2 were used. Immunoblot analysis also showed that the immunoreactivities of both α- and β-syn were almost exclusively those of their monomers (Fig. 1*A*). To further analyze expression and distribution of syn proteins, double immunolabeling/LSCM was performed using at least two antibodies for each syn (Fig. 1*B*). The immunoreactivity of α-syn in α-syn-overexpressing cells (α1) was diffuse in the cell bodies as detected by both monoclonal syn-1 and polyclonal C-terminal antibodies (*a* and *b*). Immunoreactivity of β-syn in β-syn-overexpressing cells (β5) was also localized diffusely in the cell bodies by monoclonal anti-β-syn antibody (*e*) but was detected with a shift to perinuclear regions by polyclonal anti-β-syn antibody (*f*). In none of these cases, inclusion bodies were detected. Notably, expression levels of α-syn were heterogeneous (*c*), and similar patterns were consistently observed in all the three clones of α-syn-overexpressing cells (data not shown). By contrast, immunoreactivities of β-syn were homogeneous in β-syn-overexpressing cells (*g*). No immunoreactivities of syn proteins were detected in vector-transfected cells (v2) (*d* and *h*).

To determine whether cell proliferation was affected by overexpression of syn, the stable clones were evaluated for their cell growth rates. The doubling times of cells in log phase of growth under 10% serum conditions were 20–24 h for α-syn-overexpressing cells and 14–17.5 h for both β-syn-overexpressing and vector-transfected cells (data not shown). Cells were then incubated under the low serum (0.1%) for 24 h to synchronize at G_1 in cell cycle and then added with 10% serum followed by counting of cell numbers at the indicated times. The result showed that that the average cell numbers of α-syn-overexpressing cells at day 4 were significantly decreased compared with both β-syn-overexpressing and vector-transfected cells (Fig. 1*C*).

To determine whether decreased cell proliferation of α-syn-overexpressing cells is due to alteration of cell cycle profile, cell cycle analysis was performed using flow cytometry at varying time periods (0, 6, 12, 18, 24, and 96 h) after the addition of 10% serum to serum-deprived cells. The result showed that compared with both β-syn-overexpressing and vector-transfected cells, α-syn cells in G_0/G_1 phases were significantly increased ($p < 0.05$), whereas those in both S and G_2/M phase were decreased at 24 and 96 h ($p < 0.05$) (Fig. 1*D*). Essentially similar results were observed at 96 h. However, compared with the profile at 24 h, there were more cells in G_0/G_1 phase, fewer cells in S phase, and more cells in G_2/M at 96 h. One possible reason for the difference between 24 and 96 h could be that at 24 h many cells might have not yet reached G_2/M phase. Furthermore, a relatively high ratio of cells in G_0/G_1 phase at 96 h could

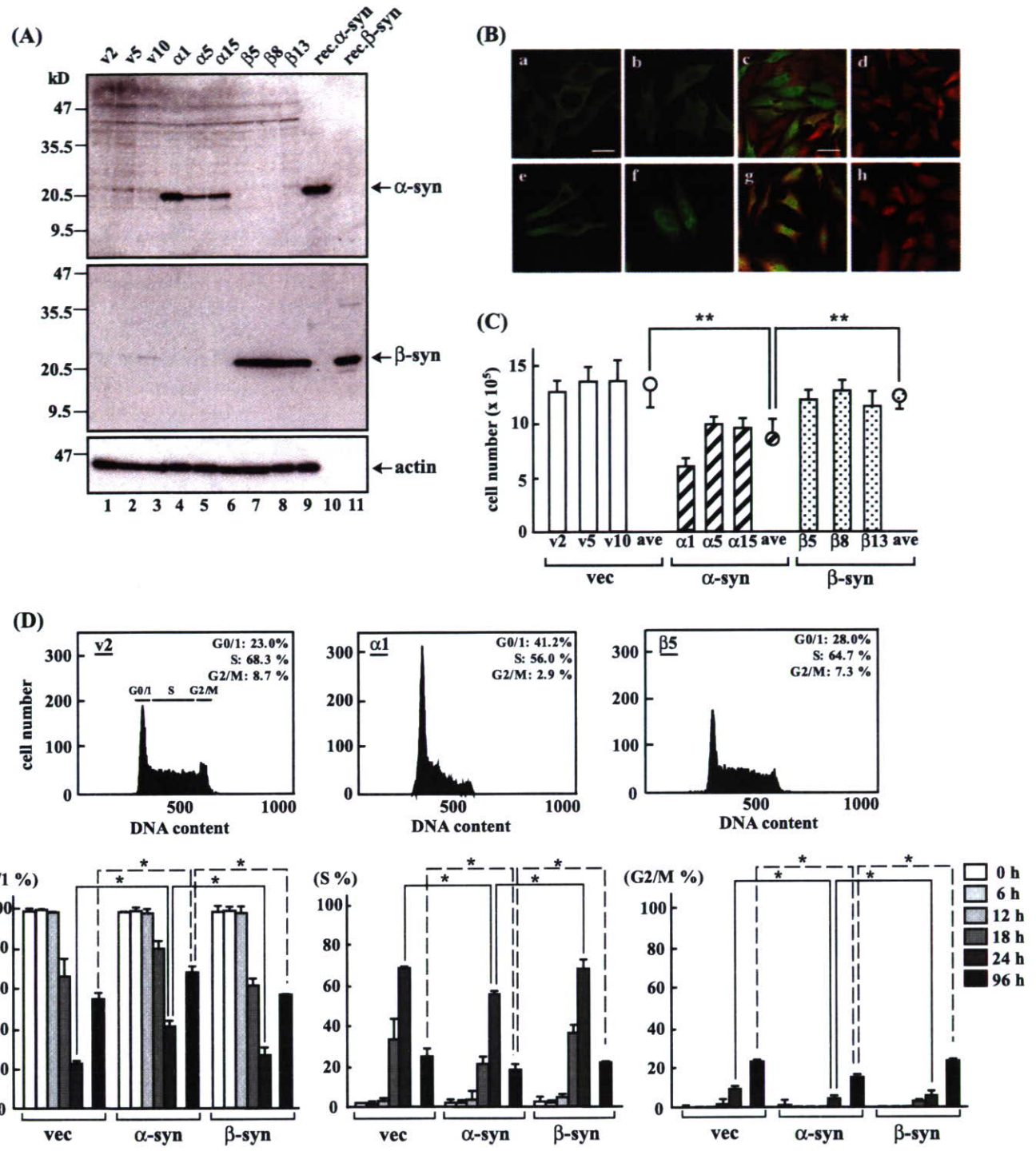

FIGURE 1. **Analysis of syn expression in transfected MG63 osteosarcoma cells.** *A*, immunoblot analysis of syn proteins. Cell extracts were analyzed by immunoblotting using syn-1 (*upper panel*), anti-β-syn monoclonal antibody (*middle panel*), and anti-actin antibody (*lower panel*). Three vector-transfected clones (v2, v5, v10, *lanes 1–3*), three high expresser clones for α-syn (α1, α5, α15, *lanes 4–6*), and β-syn (β5, β8, β13, *lanes 7–9*) are shown. Recombinant α- and β-syn proteins were used as positive controls (*lanes 10* and *11*). *B*, immunofluorescence/LSCM analysis of syn expression. α-Syn-overexpressing cells (α1) (*a–c*), β-syn-overexpressing cells (β5) (*e–g*), and vector-transfected cells (v2) (*d* and *h*) were immunostained with antibodies against α-syn (*green*, *a–d*), β-syn (*green*, *e–h*), and actin (*red*, *c*, *d*, *g*, and *h*) followed by observation by LSCM. α-Syn was diffusely distributed in the cell bodies with a slight shift to cell membrane as detected by both syn-1 (*a*) and polyclonal c-terminal antibody (*b*). β-Syn was similarly detected in the cell bodies by monoclonal anti-β-syn antibody (*e*), but strong stains of perinuclear regions were observed by polyclonal anti-β-syn antibody (*f*). Immunoreactivities of α-syn were heterogeneous (*c*), whereas those of β-syn were almost even in all cell populations (*g*). No immunoreactivities of syn proteins were detected in vector-transfected cells (*d* and *h*). *Bars* represent either 20 μm for high magnification (*a*, *b*, *e*, and *f*) or 50 μm for low magnification (*c*, *d*, *g*, and *h*). *C*, evaluation of cell proliferation. Cells (v2, v5, v10, α1, α5, α15, β5, β8, and β13) were incubated at 1×10^5 cells/well in the 6-well plates under the low serum (0.1%) conditions for 24 h to synchronize. Cells were then treated with 10% serum, and cell numbers were counted at 96 h. *Open circles* represent the group mean values. Data shown are the mean ± S.D. ($n = 3$). **, $p < 0.01$. *D*, flow cytometry for cell cycle analysis. Cells were prepared as described in *C*, and DNA contents were analyzed at the indicated times (0, 6, 12, 18, 24, and 96 h) after serum stimulation. The *upper figures* are a typical cell cycle profile at 24 h for v2, α1, and β5. The *x* axis represents the fluorescent intensities proportional to the amount of DNA, whereas the *y* axis indicates the cell number. The *lower column figures* show that G_0/G_1 phases at 24 and 96 h in α-syn cells were significantly increased, whereas those in both S and G_2/M phase were decreased compared with both β-syn-overexpressing and vector-transfected cells. Data presented are the mean ± S.D. of triple determinations. *, $p < 0.05$.

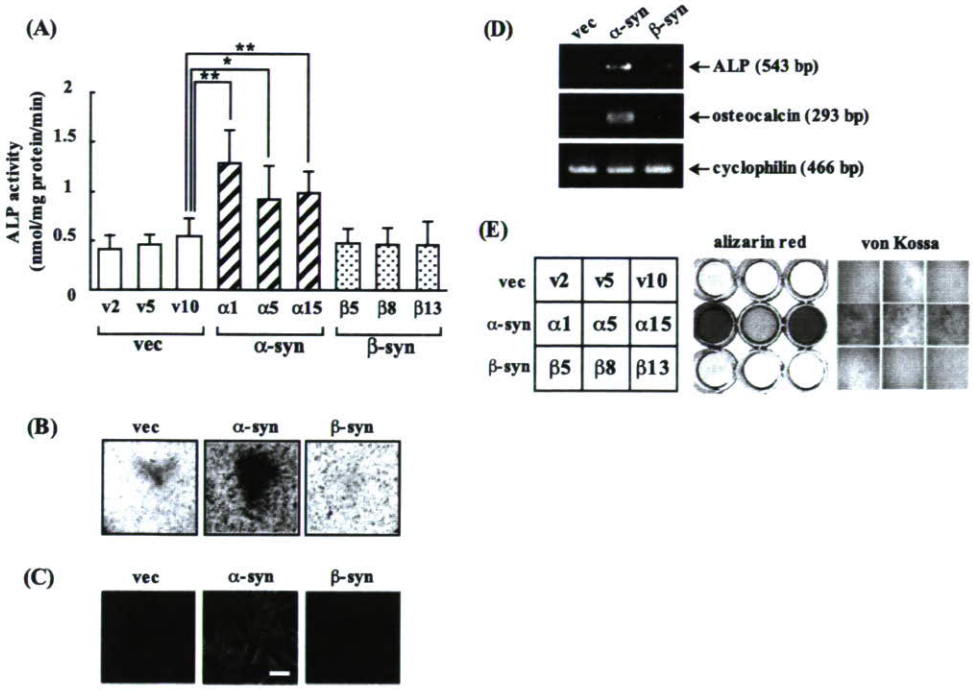

FIGURE 2. **Up-regulation of the expression of osteoblastic differentiation markers in α-syn-overexpressing MG63 cells.** *A*, measurement of ALP activity. Cells (v2, v5, v10, α1, α5, α15, β5, β8, and β13) under the confluent conditions were harvested, and cell extracts were incubated with *p*-nitrophenyl phosphate at 37 °C for 90 min. The amount of released nitrophenol was monitored by absorbance at 415 nm. α-Syn-overexpressing cells (α1) showed significantly higher ALP activity compared with other cell types (v2 and β5). Data shown are mean ± S.D. ($n = 5$). *, $p < 0.05$; **, $p < 0.01$. *B*, evaluation of ALP activity by staining. Cells (v2, α1, and β5) were stained with nitro blue tetrazolium chloride/5-bromo-4-chloro-3-indolyl phosphate solution and photographed. *C*, immunostaining of osteocalsin. Cells (v2, α1, and β5) were immunostained with anti-osteocalsin antibody followed by observation with LSCM. The *bar* represents 50 μm. *D*, RT-PCR analysis of ALP and osteocalcin mRNAs. Cyclophilin mRNA was used as an internal control. *E*, *in vitro* mineralization assay. Cells (v2, v5, v10, α1, α5, α15, β5, β8, and β13) were seeded onto 24-well cell culture plates (1×10^5 cells/ml) and maintained in α-minimal essential medium containing 10 mM β-glycerophosphate and 50 μg/ml ascorbic acid for 4 weeks. Matrix mineralization was evaluated by either alizarin red staining (*middle panel*) or von Kossa staining (*right panel*). Each clone number is indicated in the squire matrix (*left panel*). Please note that the strongest staining was observed in clone α1, the highest α-syn expresser.

be due to the decreased nutrients in the culture medium after long time culture. Taken together, these results suggested that overexpression of α-syn, but not of β-syn, suppressed cell proliferation in MG63 osteosarcoma cells.

α-Syn-overexpressing MG63 Cells Exhibit Enhanced Differentiation Phenotype—Based on the apparent decrease of growth rates and enhanced G_0/G_1 phases in cell cycle in α-syn-overexpressing MG63 cells compared with β-syn-overexpressing and vector-transfected cells, we speculated that the former cells might be shifted to cellular differentiation.

To test this possibility, we evaluated ALP since this molecule had been widely used as a marker for osteoblastic differentiation. As we suspected, all three clones of α-syn-overexpressing cells displayed significantly higher activity of ALP compared with both β-syn-overexpressing and vector-transfected cells (Fig. 2*A*). Activation of ALP was also assessed by direct stain of cells using nitro blue tetrazolium chloride/5-bromo-4-chloro-3-indolyl phosphate as substrate. The result showed that the intensity of the staining in α-syn-overexpressing cells was much stronger than those of β-syn-overexpressing and vector-transfected cells (Fig. 2*B*). Next, we analyzed expression of osteocalcin, another marker for osteoblastic differentiation. The immunofluorescence/LSCM study showed that immunoreactivity of osteocalcin was strongly observed in α-syn-overexpressing cells but not in other cell types (Fig. 2*C*). Furthermore, RT-PCR analysis revealed that up-regulation of ALP and osteocalcin in α-syn-overexpressed cells might be attributed to increased transcription (Fig. 2*D*). To further corroborate that cellular differentiation is accelerated in α-syn-overexpressing cells, we evaluated formation of mineral deposition in the matrix that may mimic the calcification by osteoblasts *in vivo*. For this purpose, cells were incubated in the presence of β-glycerophosphate and ascorbic acid for 4 weeks followed by staining with alizarin red to assess calcium incorporation. The result showed that mineralization was clearly detectable in α-syn-overexpressing cells but not in β-syn-overexpressing nor vector-transfected cells (Fig. 2*E*). Similar results were obtained by von Kossa staining for the assessment of bone nodule formation (Fig. 2*E*). Taken together, α-syn-overexpressing cells specifically exhibited a differentiated phenotype compared with both β-syn-overexpressing and vector-transfected cells.

Alteration of G_1 Cell Cycle Regulators and Decreased Proteasome Activity in α-Syn-overexpressing MG63 Cells—Because prolonged G_1 period in cell cycle is prerequisite for cell entry into G_0 and further differentiation, it was predicted that expressions and activities of various G_1 cell cycle regulators might be altered in α-syn-overexpressing cells.

To test this possibility, cells were incubated under the low serum (0.1%) conditions for 24 h to synchronize at G_1 followed by 10% serum treatment. Cells were then harvested, and expression of various cell cycle regulators were analyzed at the indicated times (Fig. 3*A*). Notably, expression of the cyclin-dependent kinase inhibitor p21, one of the key molecules which negatively regulate cell cycle progression from G_1 to S phase, was significantly up-regulated in α-syn-overexpressing cells. In these cells p21 was constitutively expressed without serum stimulation and was further increased in response to serum, reaching the maximum around 6- 12 h followed by gradual decrease. By contrast, in vector-transfected cells expression of p21 was transiently up-regulated at 6 h and immediately decreased. Consistent with this, phosphorylation of Rb protein was compromised in α-syn-expressing cells compared with vector-transfected cells. Furthermore, cyclin B1, a marker for G_2/M phase, was up-regulated earlier in vector-transfected cells than in α-syn-overexpressing cells. As for other cyclin-dependent kinase inhibitors, p15 level was slightly elevated at 24- and 48-h time points, whereas expression of p27 was not up-

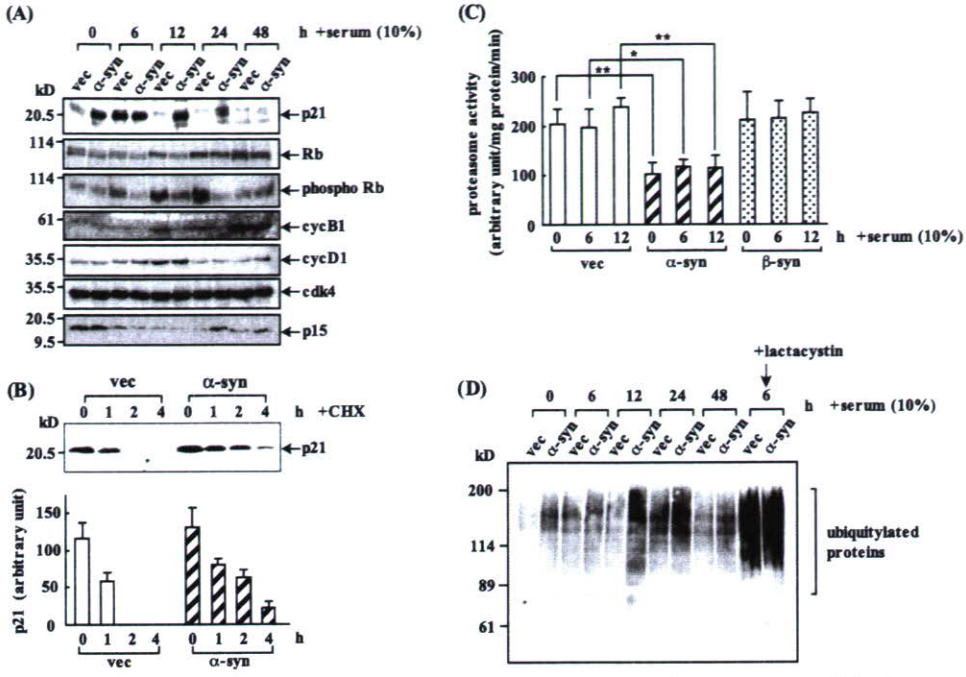

FIGURE 3. **Altered expression of cell cycle regulators and decrease of proteasome activity in α-syn-overexpressing MG63 cells.** *A*, immunoblot analysis of cell cycle regulators. Vector-transfected (v2) and α-syn-overexpressing cells (α1) were incubated under the low serum (0.1%) conditions for 24 h to synchronize and then treated with 10% serum for the indicated times (6, 12, 24, and 48 h). Cells were then harvested, and cell lysates were analyzed by immunoblotting with anti-p21, Rb, phospho Rb, cyclin (*cyc*) B, cyclin D1, cyclin-dependent kinase (*Cdk4*), p15, and ubiquitin. *B*, evaluation of the stability of p21 protein by cycloheximide experiments. The synchronized cells (v2 and α1) were treated with 10% serum with or without cycloheximide (*CHX*) for the indicated times (1, 2, and 4 h), and cell lysates were analyzed by immunoblotting (*upper panel*). Each band was quantified using BioMax 1D image analysis soft ware (*lower panel*). Data shown are the mean ± S.D. Similar results were obtained by three independent experiments. *C*, measurement of proteasome activity. Cells (v2, α1, and β5) were incubated under the low serum (0.1%) conditions for 24 h and then treated with 10% serum for the indicated times (6 and 12 h). To evaluate proteasome activity, cell extracts (10 μg) were incubated with fluorogenic substrate (benzyloxycarbonyl-Leu-Leu-Glu-amidomethylcoumarin) at 37 °C. Released fluorescence (excitation 380 nm, emission 460 nm) was monitored by 5 min intervals up to 60 min. The fluorogenic value at each time point was plotted, and the slope was calculated. Data shown are the mean ± S.D. ($n = 3$). *, $p < 0.05$; **, $p < 0.01$. *D*, immunoblot analysis of ubiquitylated proteins. Vector-transfected (v2) and α-syn-overexpressing cells (α1) were prepared as described in *A* and analyzed by immunoblotting using anti-ubiquitin antibody. Both types of cells treated with lactacystin for 6 h were included as positive controls.

regulated in α-syn-overexpressing cells compared with vector-transfected cells (Fig. 3*A* and data not shown). Expression of other cell cycle regulators such as cyclin D1 and cyclin-dependent kinase 4 were not much different between both cell types. Similar expression patterns of p21 and phosphorylated Rb were observed between β-syn-overexpressing cells and vector-transfected cells (data not shown).

Next, to determine whether up-regulation of p21 expression was due to the stabilization of p21 protein in α-syn-overexpressing cells, these cells were treated with cycloheximide to inhibit protein synthesis 6 h after serum stimulation. Under these conditions, expression levels of p21 protein quickly decreased within 2 h of treatment in vector-transfected cells, whereas expression levels in α-syn-overexpressing cells took longer to detect (Fig. 3*B*). Under the same experimental conditions, p21 mRNA was evaluated by real time PCR. However, no significant differences were observed between α-syn-overexpressing and vector-transfected cells (data not shown).

To further determine whether increased stability of p21 was due to compromised degradation by UPS in α-syn-overexpressing cells, syn-transfected cells were analyzed for proteasome activities. The result showed that the proteasome activities of α-syn-overexpressing cells were decreased to ~50% of those of vector-transfected cells, whereas those of β-syn-overexpressing cells were little affected (Fig. 3*C*). Under the same experimental conditions, immunoreactivities of polyubiquitylated proteins were significantly stronger in α-syn-overexpressing cells compared with those in vector-transfected and β-syn-overexpressing cells (Fig. 3*D* and data not shown). Taken together, expression of cell cycle regulators such as p21 and phosphorylated Rb were altered in α-syn-overexpressing cells, which might be attributed to the decreased proteasome activity.

Proteasome Inhibitors Stimulate Differentiation of Wild-type MG63 Cells—If suppression of proteasome activity by α-syn plays a causative role for stimulation of differentiation in MG63 osteosarcoma cells, then it is possible that down-regulation of proteasome activity by other experimental procedures might similarly stimulate differentiation in these cells.

To test this possibility, wild-type MG63 cells were treated with proteasome inhibitors, including MG132 and lactacystin followed by evaluation of cellular differentiation. Immunoblot analysis revealed that administration of these reagents at 10 μM clearly up-regulated p21 expression at 12 h (Fig. 4*A*). Under the same experimental conditions, ALP activity was significantly up-regulated, and immunoreactivity of osteocalcin became detectable (Fig. 4*B* and data not shown). In addition, the expression of ALP and osteocalcin mRNA was up-regulated in lactacystin-treated cells (Fig. 4*C*). Furthermore, cells were induced to form matrix mineralization with lower concentrations of proteasome inhibitors (0.01–0.1 μM for MG132 and 0.1–1.0 μM for lactacystin) in long-term cultures. High concentration (10 μM) treatment of these reagents caused prominent cell death within 48 h (data not shown). By contrast, sublethal concentrations (0.01–0.1 μM) of rotenone, an inhibitor of mitochondria complex I, caspase I, and III inhibitors (0.1–1.0 μM), and leupeptin (1–10 μM) had little effect on cellular differentiation (Fig. 4*D*). Taken together, treatment of wild-type MG63 cells with proteasome inhibitors resulted in stimulation of cellular differentiation.

Down-regulation of PKC Activity in α-Syn-overexpressing MG63 Cells—Our hypothesis was that alteration of signal transduction might be involved in the suppression of proteasome activity in α-syn-overexpressing cells. In this regard we especially focused on the potential role of PKC since it was recently shown that treatment of skeletal muscle by phorbol

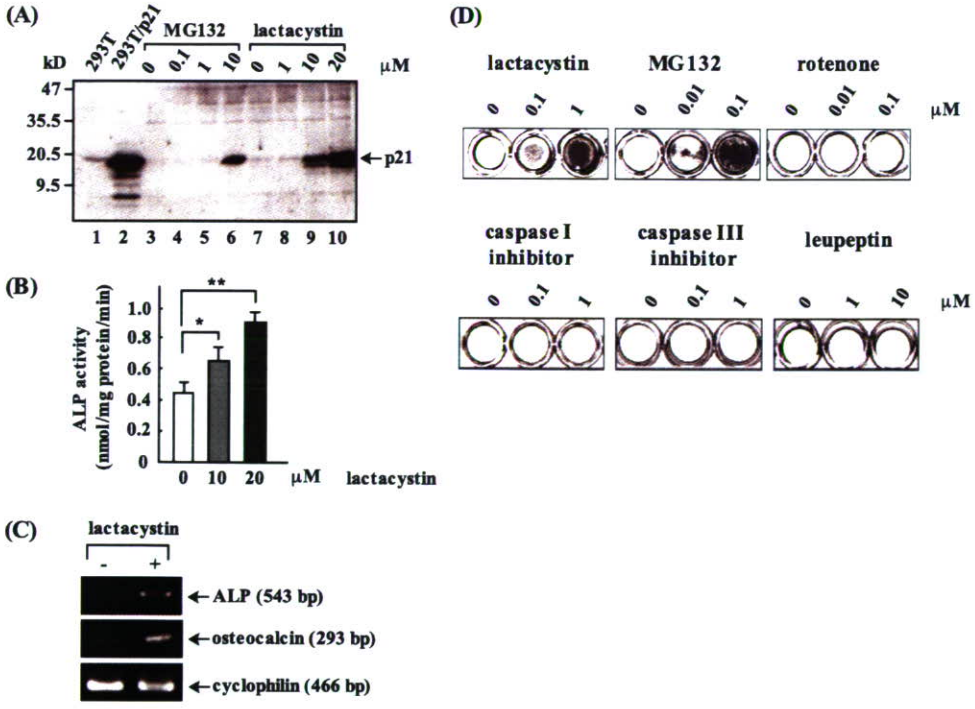

FIGURE 4. **Proteasome inhibitors induce cellular differentiation in wild-type MG63 cells.** Wild-type MG63 were incubated under the low serum (0.1%) conditions for 24 h and then treated with 10% serum in the presence of either MG132 or lactacystin. *A*, immunoblot analysis of p21. Cells were treated with various concentrations of either MG132 (0, 0.1, 1.0, 10 μM, *lanes 3–6*) or lactacystin (0, 1.0, 10, 20 μM, *lanes 7–10*) and harvested at 12 h. Cell lysates were analyzed by immunoblotting using anti-p21 antibody. Extracts of 293T cells transfected with or without p21 expression vector are shown as controls (*lanes 1* and *2*). *B*, measurement of ALP activity. Cells were treated with various concentrations (0, 10, 20 μM) of lactacystin for 12 h. To evaluate ALP activity, cell extracts were incubated with *p*-nitrophenyl phosphate at 37 °C for 90 min. The amount of released nitrophenol was monitored by the absorbance at 415 nm. Data shown in the *left panel* are the mean ± S.D. ($n = 3$). *, $p < 0.05$; **, $p < 0.01$. *C*, RT-PCR analysis of ALP and osteocalcin mRNAs. Cells were treated with lactacystin (10 μM) for 24 h. Cyclophilin mRNA was used as an internal control. *D*, *in vitro* mineralization assay. Cells were treated with various reagents, including MG132 (0, 0.01, 0.1 μM), lactacystin (0, 0.1, 1.0 μM), rotenone (0, 0.1, 0.1 μM), caspase I inhibitor (0, 0.1, 1.0 μM), caspase III inhibitor (0, 0.1, 1.0 μM), and leupeptin (0, 1, 10 μM) for 4 weeks. Matrix mineralization was evaluated by alizarin red staining. Please note that positive staining was observed for cells treated with proteasome inhibitors. Acridine orange/ethidium bromide staining revealed that cells were alive during mineralization (not shown).

ester resulted in stimulation of proteasome activity (39) and it was previously shown that α-syn bound with PKC and down-regulated the activity of PKC in α-syn overexpressing neuroblastoma cells (40).

To determine whether α-syn associates with PKC, a co-immunoprecipitation experiment was performed (Fig. 5*A*). Cell extracts of α-syn-overexpressing cells were immunoprecipitated with syn-1 followed by immunoblotting analysis with mouse anti- PKCε antibody. In agreement with a previous study by Ostrerova *et al.* (40), the result showed that PKCε was specifically co-immunoprecipitated with α-syn.

Next, to further determine whether α-syn colocalize with PKC, cells were double-immunolabeled with anti-α-syn rabbit polyclonal antibody and anti-PKCε antibody followed by observation with LSCM. As shown in Fig. 5*B*, immunoreactivities of α-syn and PKCε considerably overlapped in the cytoplasm of α-syn-overexpressing cells. We observed that PKCε and PKCλ were highly expressed in addition to moderate expression of other PKC family of peptides in MG63 cells (data not shown). Similar results were obtained by both co-immunoprecipitation and double immunolabeling/LSCM studies for PKCλ (data not shown).

Finally, to determine whether PKC activity was compromised in α-syn-overexpressing cells, the syn-transfected cells were treated with or without PMA and analyzed for their PKC activities (Fig. 5*C*). The result showed that proteasome activities of α-syn-overexpressing cells were significantly lower than those of β-syn-overexpressing and vector-transfected cells. Importantly, PMA treatment of α-syn-overexpressing cells restored the PKC activity to the basal levels of those in other cell types. Taken together, these results suggested that α-syn might directly suppress the PKC activity in α-syn-overexpressing cells.

Because previous studies suggested an alternative possibility that α-syn bound with S6 subunit of 19 S proteasome, leading to interference with proteasome functions (41–43), we investigated the association of α-syn with S6a. The results of co-immunoprecipitation experiment confirmed the association of these molecules (Fig. 5*A*). Double immunolabeling/LSCM showed that overlapping of the immunoreactivities of these molecules was partially detected in the cell bodies, since S6a was considerably localized in the nucleus (Fig. 5*B*).

Phorbol Ester Treatment of α-Syn-overexpressing MG63 Cells Restores Proteasome Activity and Suppresses Cellular Differentiation—If suppression of PKC activity by α-syn is causative for down-regulation of proteasome activity and enhanced differentiation in α-syn-overexpressing cells, then stimulation of PKC might restore the proteasome activity and abrogate cellular differentiation in these cells.

Accordingly, α-syn-overexpressing cells were treated with phorbol ester followed by evaluation of proteasome activity. The results showed that the compromised activity of proteasome in α-syn-overexpressing cells was significantly improved by treatment with PMA both at 10 and 50 nM but not with an inactive analogue 4αPDD (Fig. 6*A*). On the other hand, although proteasome activity of vector-transfected cells was increased by treatment with 50 nM PMA, there were little effects observed at 10 nM PMA (Fig. 6*A*). Thus, α-syn-overexpressing cells responded more sensitively to PMA treatment, suggesting the effect of PMA on proteasome was more specific for α-syn-overexpressing cells, which showed decreased proteasome activity. The stimulatory effects of PMA on the proteasome activity in α-syn-overexpressing cells reached the maximum at 50 nM (data not shown) and were completely abro-

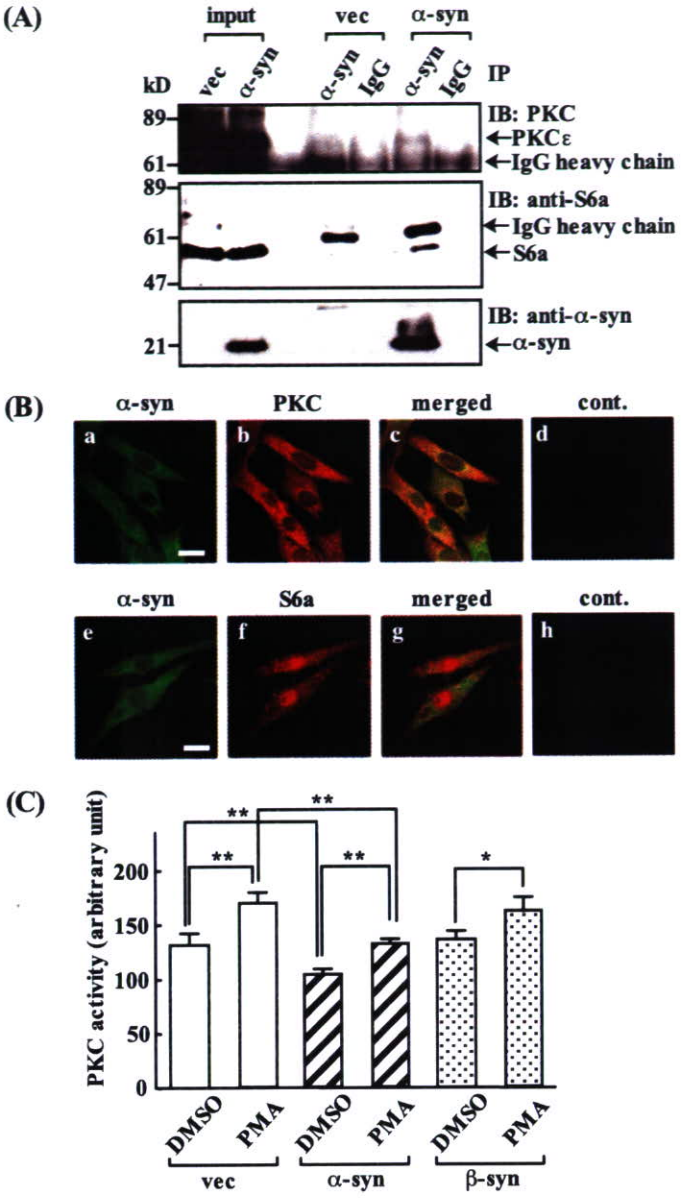

FIGURE 5. **Association of α-syn with PKC and down-regulation of PKC activity in α-syn-overexpressing MG63 cells.** *A*, coimmunoprecipitation (*IP*) of α-syn with either PKCε (*upper*) or S6a (*middle*). Vector-transfected (v2) and α-syn-overexpressing cells (α1) were harvested, and cell extracts (300 μg) were immunoprecipitated with anti-α-syn antibody or mouse IgG control followed by immunoblotting (*IB*)with either anti-PKCε (*upper*), anti-S6a (*middle*), or syn-1 (*low*). Cell extracts (5% of input) were used as positive controls. *B*, immunofluorescence/LSCM of α-syn association with either PKCε or S6a in α-syn-overexpressing cells. Cells (α1) were doubly stained with anti-α-syn antibody (*green*) and either anti-PKCε or S6a (*red*) and observed by LSCM. Please note that α-syn (*red*) and PKCε (*green*) were well co-localized in the cell bodies (*c*). *Bars* represent 50 μm. *C*, measurement of PKC activity. Exponentially growing cells (v2, α1, and β5) were treated with or without PMA for 20 min, and cell extracts (10 μg) were analyzed for PKC activity using fluorogenic peptides as substrates as described under "Experimental Procedures." Data shown are the mean ± S.D. ($n = 3$). *, $p < 0.05$; **, $p < 0.01$. *DMSO*, dimethyl sulfoxide.

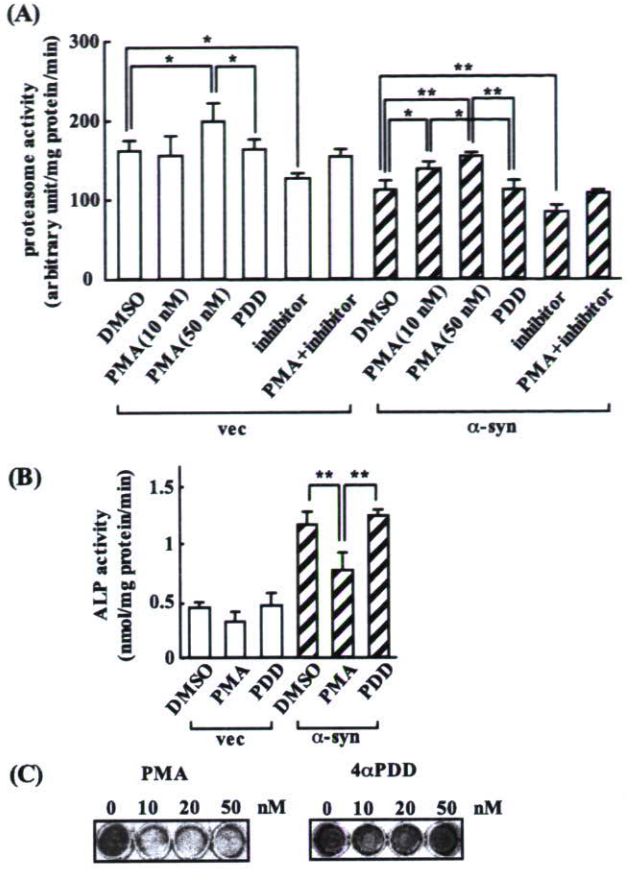

FIGURE 6. **Phorbol ester treatment restores proteasome activity and abrogates differentiation in α-syn-overexpressing MG63 cells.** *A*, measurement of proteasome activity. Vector-transfected (v2) and α-syn-overexpressing cells (α1) were incubated under the low serum (0.1%) conditions for 24 h and then treated with 10% serum in the presence of any of vehicle (0.1% Me_2SO (*DMSO*)), PMA (10 and 50 nM), 4αPDD (50 nM), chelerythrine chloride (PKC inhibitor, 50 nM), or PMA (50 nM) plus chelerythrine chloride (50 nM). Cell extracts (5 μg) were harvested at 12 h after treatment and incubated with fluorogenic proteasome substrate at 37 °C. Released fluorescence (excitation, 380 nm; emission, 460 nm) was monitored each 5 min up to 60 min. Fluorogenic intensity of each time point was plotted, and the slope was calculated. Data shown are the mean ± S.D. ($n = 3$). **, $p < 0.01$. *B*, measurement of ALP activity. Vector-transfected (v2) and α-syn-overexpressing cells (α1) were treated as described in *A*. Cell extracts at 12 h treatment were incubated with *p*-nitrophenyl phosphate at 37 °C for 90 min. The amount of released nitrophenol was monitored by the absorbance at 415 nm. Data shown are the mean ± S.D. ($n = 3$). *, $p < 0.05$; **, $p < 0.01$. *C*, *in vitro* mineralization assay. α-Syn-overexpressing cells (α1) were treated with either PMA or 4αPDD at the indicated concentrations (0, 10, 20, 50 nM). Matrix mineralization was then evaluated by alizarin red staining. Please note that the staining was mitigated by PMA but not by 4αPDD. Similar results were obtained by three independent experiments.

gated in the presence of PKC inhibitor, chelerythrine chloride (Fig. 6*A*), implying that PMA stimulated proteasome activity through phosphorylation but not through depletion of PKC.

Next, to determine whether PKC stimulation of proteasome activity modifies differentiation in α-syn-overexpressing cells, cellular differentiation markers were analyzed. Compared with treatment with either vehicle or inactive 4αPDD, PMA efficiently reduced ALP activity in α-syn-overexpressing cells (Fig. 6*B*). Immunoreactivity of osteocalcin was also decreased by PMA but not by 4αPDD in these cells (data not shown). Finally, it was confirmed that PMA, but not 4αPDD, significantly reduced matrix mineralization in α-syn-overexpressing cells as demonstrated by decreased stains of alizarin red (Fig. 6*C*). Taken together, PMA treatment of α-syn-overexpressing cells restored proteasome activity and abrogation of cellular differentiation in these cells.

Up-regulation of Lysosomal Activity in α-Syn-overexpressing MG63 Cells—Because a recent study has shown that autophagy-lysosomal pathway may play an important role for aggre-

gate-prone proteins, including α-syn and Huntingtin (44), it is reasonable to speculate that down-regulation of proteasome activity by α-syn might be further modulated by this pathway.

In this context we wondered if lysosomal activity might be altered due to increased level of α-syn expression in α-syn-overexpressing cells. To test this hypothesis, cysteine protease cathepsin B, one of the major protease in lysosome, was evaluated. The results showed that cathepsin B was significantly up-regulated in α-syn-overexpressing cells compared with vector-transfected and β-syn-overexpressing cells (Fig. 7*A*). Consistent with this, expression of cathepsin B was up-regulated at protein and mRNA levels in α-syn-overexpressing cells (Fig. 7*B*, data not shown). To investigate the ultrastructure of lysosome, an electron microscopic study was performed. The results revealed extensive lysosomal pathology, such as autolysosome and myelinosome, in α-syn-overexpressing cells (Fig. 7*C*, *a*, *c*, *e*, and *f*). On the contrary, fewer lysosomes were observed in vector-transfected and β-syn-overexpressing cells (Fig. 7*C*, *b* and *d*). Taken together, these results suggested that lysosomal activity was up-regulated in α-syn-overexpressing cells.

Autophagy-lysosomal Inhibitor Treatment Results in Down-regulation of Proteasome Activity, Leading to Acceleration of Cellular Differentiation in α-Syn-overexpressing MG63 Cells—If up-regulation of lysosomal activity in α-syn-overexpressing cells may reflect the compensatory mechanism against the increased level of α-syn, then suppression of autophagy-lysosomal pathways may result in compromised clearance of α-syn, leading to decrease proteasome activity and accelerate cellular differentiation in those cells.

We first evaluated expression levels of α- and β-syn proteins in the presence of autophagy-lysosomal inhibitors. The results of immunoblot analysis showed that α- and β-syn proteins were up-regulated by macroautophagy inhibitor 3-MA as well as by ammonium chloride, which inhibits lysosomal activity independently of the form of autophagy. By contrast, proteasome inhibitor lactacystin had little effect on the expression of both α- and β-syn proteins (Fig. 8*A*). Thus, these results suggested that α- and β-syn were preferentially degraded by autophagy-lysosomal pathway.

Then, to determine whether down-regulation of autophagy-lysosomal activity affects proteasome function, proteasome activity was evaluated by treatment with autophagy-lysosomal inhibitors. The result showed that treatments with autophagy-lysosomal inhibitors significantly decreased proteasome activities in α-syn-overexpressing cells but not in other cell types (Fig. 8*B*). By contrast, inhibition of proteasome by lactacystin had little effect on cathepsin B activity (data not shown). Similarly, treatment of PMA, which was shown to stimulate proteasome activity (Fig. 6), had little effects on cathepsin B activity (data not shown).

Finally, it was shown that treatment with both 3-MA and ammonium chloride significantly stimulated ALP activity, osteocalcin expression, and matrix mineralization in α-syn-overexpressing cells compared with other cell types (Fig. 8, *C* and *D*, data not shown). Taken together, inhibition of autophagy-lysosomal activity in α-syn-overexpressing cells resulted in down-regulation of proteasome activity, leading to stimulate

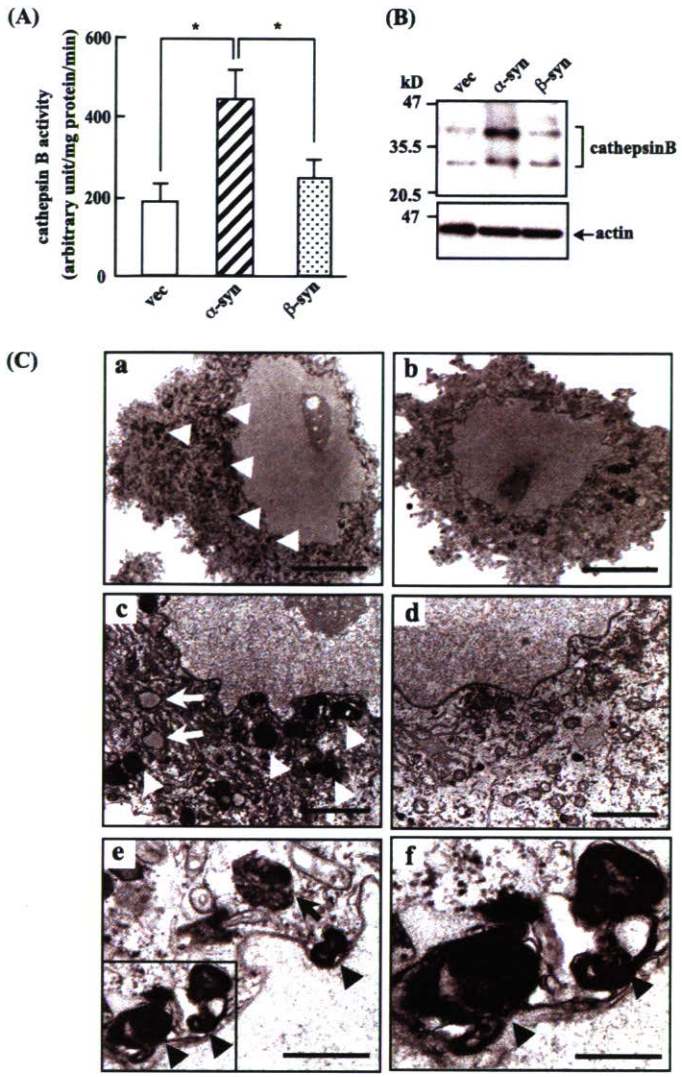

FIGURE 7. **Up-regulation of lysosomal activity in α-syn-overexpressing MG63 cells.** *A*, measurement of cathepsin B activity. Cell extracts (10 μg) were prepared as described under "Experimental Procedures" were analyzed for cathepsin B activity using fluorogenic substrates. Released fluorescence (excitation, 380 nm; emission, 460 nm) was monitored each 5 min up to 60 min. Fluorogenic intensity of each time point was plotted, and slope was calculated. Data shown are the mean ± S.D. ($n = 3$). *, $p < 0.05$; **, $p < 0.01$. *B*, immunoblot analysis of cathepsin B. Cell extracts (v2, α1, and β5) were analyzed by immunoblotting using anti-cathepsin B antibody (*upper panel*) and anti-actin antibody (*lower panel*). *C*, electron microscopic analysis. Typically, α-syn-overexpressing cells (α1: *a*, *c*, *e*, and *f*) exhibited numerous enlarged electron-dense lysosomes (*white arrowheads*), vacuoles that might have already discharged their contents (*white arrows*), autolysosome-like body (*black arrow*), and myelinosome-like structures (*black arrowheads*). The enclosed area in *panel e* is magnified in *panel f*. Fewer lysosomal structures were found in vector-transfected cells (v2, *b*) and β-syn-overexpressing cells (β5, *d*). *Bars* represent 8 μm (*a* and *b*, x1500), 2 μm (*c* and *d*, ×5000), 1 μm (*e*, ×13000), or 0.5 μm (*f*, ×26000).

cellular differentiation. Thus, these results suggest that autophagy-lysosomal pathway may mitigate the down-regulation of proteasome activity by α-syn, therefore leading to abrogate cellular differentiation by α-syn.

DISCUSSION

Although α-syn was previously shown to be expressed in the brain tumors that preferentially displayed differentiation rather than proliferation, little has been documented regarding the role of

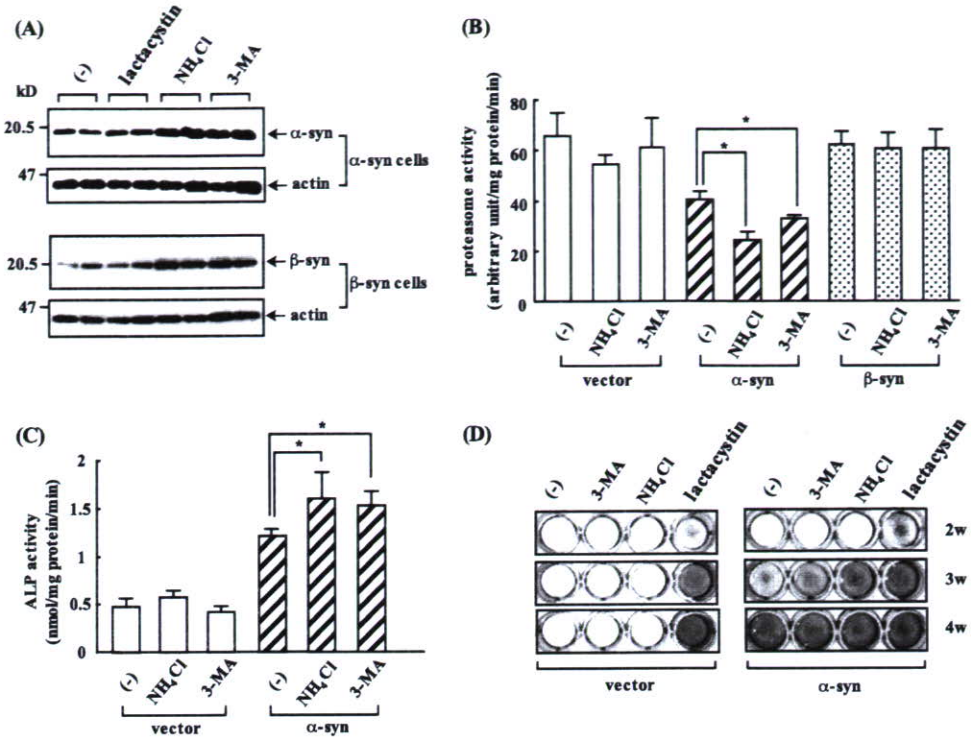

FIGURE 8. **Autophagy-lysosome inhibitor treatment decreases proteasome activity and stimulates cellular differentiation in α-syn-overexpressing MG63 cells.** *A*, immunoblot analysis of syn proteins. Cells (α1, and β5) were incubated under the low serum (0.1%) conditions for 24 h and then treated with 10% serum in the presence of lactacystin (10 μM), ammonium chloride (NH_4Cl) (20 mM), and 3-MA (10 mM) for 24 h. Cell lysates were analyzed by immunoblotting using syn-1 (*upper panel*) and anti-β-syn monoclonal antibody (*low panel*). Blots were reprobed with anti-actin antibody. Similar results were obtained by three independent experiments. *B*, measurement of proteasome activity. Cells (v2, α1, and β5) were prepared as described in *A*. Cell extracts (5 μg) were harvested and incubated with fluorogenic proteasome substrate at 37 °C. Released fluorescence (excitation, 380 nm; emission, 460 nm) was monitored each 5 min up to 60 min. Fluorogenic intensity of each time point was plotted, and slope was calculated. Data shown are the mean ± S.D. ($n = 3$). Please note that proteasome activity was significantly decreased in α-syn-overexpressing cells by ammonium chloride treatment (*, $p < 0.05$). *C*, measurement of ALP activity. Vector-transfected (v2) and α-syn-overexpressing cells (α1) were prepared as described in *A*. Cell extracts at 12 h of treatment were incubated with *p*-nitrophenyl phosphate at 37 °C for 90 min. The amount of released nitrophenol was monitored by the absorbance at 415 nm. Data shown are the mean ± S.D. ($n = 3$). *, $p < 0.05$; **, $p < 0.01$. *D*, *in vitro* mineralization assay. Vector-transfected (v2) and α-syn-overexpressing cells (α1) were treated with ammonium chloride (10 mM), 3-MA, (10 mM), or lactacystin (1 μM) for 2–4 weeks (*2W–4W*). Matrix mineralization was then evaluated by alizarin red staining. Please note that the staining was stimulated by ammonium chloride and to a lesser extent by 3-MA in α-syn-overexpressing cells but not in vector-transfected cells. Similar results were obtained by three independent experiments.

α-syn for tumor differentiation. The present study showed that α-syn-overexpressing MG63 osteosarcoma cells specifically exhibited phenotype of osteoblastic differentiation. Compared with both β-syn-overexpressing and vector-transfected cells, α-syn-overexpressing cells were characterized by decreased growth rates, associated with increased expression of p21 and reduced phosphorylated Rb (Figs. 1 and 3), indicating that the progression from G_1 to S phase was compromised in these cells. The prolonged G_1 phase would be prerequisite for transition from G_1 to G_0 and subsequent cellular differentiation. Consistent with this view, osteoblastic differentiation markers, including ALP and osteocalcin, were significantly up-regulated in α-syn-overexpressing cells compared with other cell types (Fig. 2). Furthermore, α-syn-overexpressing cells, but not other cell types, were induced to form matrix mineralization during long-term cultures (Fig. 2). Taken together, our results using osteosarcoma cells support the contention that α-syn might stimulate tumor differentiation.

Because proteasome activity was significantly lower in α-syn-overexpressing cells compared with both β-syn-overexpressing and vector-transfected cells (Fig. 3), it was assumed that down-regulation of proteasome activity by α-syn could be at play for accelerated cellular differentiation in α-syn-overexpressing cells. Supporting this notion, expression levels of p21 were up-regulated due to increased stability at the protein level. Furthermore, high molecular weight proteins with polyubiquitylation were also significantly accumulated (Fig. 3). Thus, it was interpreted that decreased proteasome activity might result in prolonged G_1 phase of cell cycle, which could be prerequisite for proliferating cells to escape from cell cycle and proceed to differentiation. Indeed, it has been well described that proteasome inhibitors stimulated cellular differentiation in a variety of cell types, including osteoblastic cells (45), PC12 cells (46, 47), and oligodendrocytes (48). For example, proteasome inhibitors induced osteoblastic differentiation and bone formation *in vitro* and *in vivo*, which were associated with up-regulation of bone morphogenetic protein-2 (45). It was also shown that proteasome inhibitors stimulated neurite outgrowth in PC12 cells through activation of c-Jun NH_2-terminal kinase signaling pathway (46, 47). We also confirmed that treatment of wild-type MG63 cells with proteasome inhibitors, such as MG132 and lactacystin, resulted in similar differentiation phenotype as characterized by increased expression of p21, up-regulation of ALP and osteocalcin, and enhanced matrix mineralization (Fig. 4).

Then, what is the mechanism through which α-syn suppresses proteasome activity? In this regard several reports have already documented a possibility that α-syn may directly interfere with the proteasome. Based on two-hybrid screening, α-syn was shown to bind to S6′, a component of the 19 S subunit in the 26 S proteasome, in cell cultures (41). Subsequently, it was shown that aggregated α-syn, but not its monomeric form, efficiently inhibited the activity of the 26 S proteasome under the cell-free conditions (42, 43, 49). Using α-syn-overexpressing MG63 cells, we observed that S6a was co-precipitated with α-syn by co-immunoprecipitation experiment, although immunofluorescence/LSCM study revealed that these molecules were partially colocalized in the cytoplasm (Fig. 5). Although we failed to observe any evidence of aggregated α-syn by both immunoblotting and immunofluorescence/LSCM (Fig. 1*B*, *a* and *b*), one possible explanation for supporting the pos-

sibility of the direct suppression of proteasome by α-syn could be that misfolded monomer of α-syn rather than SDS-resistant oligomers/high molecular aggregates might be at play for the suppression of proteasome functions in α-syn-overexpressing MG63 cells. In contrast to α-syn, β-syn, a less aggregate-prone protein that is non-amyloidogenic under the physiological conditions, had little effect on proteasome activity. The result is consistent with the previous report by Snyder *et al.* (49).

An alternative possibility that we favor is that alteration of signal transduction might play an important role for suppression of proteasome activity in α-syn-overexpressing cells. Indeed, it has been shown that various signaling molecules in mitogen-activated protein kinase and phosphatidylinositol 3-kinase pathways were altered by accumulation of α-syn in a variety of cell cultures (35, 50). In the present study the role of the PKC signaling pathway was addressed for the regulation of proteasome activity because it was recently shown that treatment of skeletal muscle with phorbol ester stimulated proteasome activity (39). Consistent with a previous study using neuroblastoma cells and human brains (40), α-syn was shown to bind with PKC, thereby down-regulating the activity of this molecule in α-syn-overexpressing MG63 cells (Fig. 5). Furthermore, treatment of α-syn-overexpressing cells with PMA significantly restored the proteasome activity and abrogated differentiation in these cells (Fig. 6). Thus, proteasome activities were inversely correlated with the extent of differentiation, reinforcing the concept that suppression of proteasome activity by α-syn may accelerate differentiation. Although the precise mechanism by which the proteasome is activated by PKC stimulation requires further investigation, it is possible that phosphorylation might be involved. Supporting this notion, it was recently shown that phosphorylation of α subunits of 20 S proteasome by various stimuli, such as γ-interferon and casein kinase II, was important for the regulation of the stability of 26 S proteasome complexes in mammalian cells (51). Taken together, proteasome activity may be regulated through phosphorylation by signal transduction pathways, including PKC, which may be down-regulated by accumulation of α-syn.

Given the emerging role of autophagy-lysosomal pathway for the degradation of α-syn (52, 53), it is probable that alteration of this pathway may affect α-syn-mediated suppression of proteasome activity. Indeed, the present study showed that the lysosomal activity was significantly up-regulated in α-syn-overexpressing cells compared with other cells (Fig. 7). Furthermore, in α-syn-overexpressing cells, inhibition of the autophagy-lysosomal pathway resulted in down-regulation of proteasome activity associated with up-regulation of α-syn, whereas inhibition of proteasome activity had little effect on autophagy-lysosomal activity with little change of α-syn, suggesting that autophagy-lysosomal pathway is dominant to negatively regulate proteasome activities in these cells (Fig. 8). Together, these results suggest that lysosomal activity was up-regulated due to the compensatory mechanisms against increased level of α-syn. It has been recently shown that the autophagy-lysosomal pathway has pleiotropic roles in the regulation of cancer (54). For example, this pathway may be indispensable to tumors that must frequently survive under the nutrient-poor environments. Conversely, loss of function of this pathway might be beneficial because of accumulation of genotoxic substances in the cytoplasm that could promote mutation and, hence, tumorigenesis. The present study may provide a novel mechanism that the autophagy-lysosomal degradation pathway might negatively modulate the UPS-regulated cellular differentiation in α-syn-overexpressing tumors.

Because the identification of gene mutations of parkin in recessive familial PD and further characterization of this molecule as a ubiquitin E3 ligase, it has been extensively shown that dysfunction of UPS may be one major pathogenic pathway for PD and related neurodegenerative disorders. In this context, much literature has described that overexpression of α-syn was shown to result in decreased proteasome activities in a variety of biological system, including yeast (55) and the inducible expression system in PC12 cells (56), whereas some studies described that suppression of proteasome activity was not observed either in transgenic mice or in some cell cultures, including PC12 and 293 cells (37). Our results are in line with the former reports and further suggest that down-regulation of UPS by α-syn may play an important role for cells to escape from cell cycle and commit to cellular differentiation. Although little has been documented regarding the role of α-syn for cell cycle, Lee *et al.* (57) previously showed that inducible expression of α-syn in PC12 cells resulted in enhanced proliferation rates through stimulation of ERK pathway whereby cells were enriched in the S phase associated with increased accumulation of cyclin B and down-regulation of Rb (57). The reason for the apparent discrepancy between the report by Lee *et al.* (57) and our present study is obscure. However, one possible explanation is that effects of α-syn on growth and differentiation might be cell type-specific. Indeed, it was shown that inducible expression of α-syn in neuro2A cells resulted in inactivation of ERK and other mitogen-activated protein kinase signals (58). Taken together, although our results using MG63 osteosarcoma cells suggest a role of α-syn for tumor differentiation, further investigation is required to confirm our current findings *in vivo*.

In conclusion, our results showed that accumulation of α-syn might result in down-regulation of proteasome activity, leading to accelerate cellular differentiation in osteosarcoma cells. This process is further modulated by various factors, including PKC signaling pathway as well as autophagy-lysosomal activity. Moreover, because a recent study has shown that many of other PD-related molecules are directly or indirectly involved in the regulation of UPS (59), it is possible that the PD-related molecules might converge to regulate the activity of UPS in tumor differentiation. Thus, comprehensive understanding of the common pathway shared by both neurodegenerative disease and cancer have a great potential to provide a novel insight into the mechanism of these distinct categories of diseases.

Acknowledgments—We thank Dr. Koji Okamoto (National Cancer Center Research Institute, Tokyo) for critical reading of the manuscript and Drs. Hidetaka Yakura and Kazuya Mizuno (Tokyo Metropolitan Institute for Neuroscience) for instructions on flow cytometry. We are also indebted to Hideki Itabashi for help in preparing the photographs.

REFERENCES

1. Hashimoto, M., and Masliah, E. (1999) *Brain Pathol.* **9,** 707–720
2. Trojanowski, J., Goedert, M., Iwatsubo, T., and Lee, V. (1998) *Cell Death Differ.* **5,** 832–837
3. Jakes, R., Spillantini, M., and Goedert, M. (1994) *FEBS Lett.* **345,** 27–32
4. Ueda, K., Fukushima, H., Masliah, E., Xia, Y., Iwai, A., Yoshimoto, M., Otero, D. A., Kondo, J., Ihara, Y., and Saitoh, T. (1993) *Proc. Natl. Acad. Sci. U. S. A.* **90,** 11282–11286
5. Lansbury, P. T., Jr. (1999) *Proc. Natl. Acad. Sci. U. S. A.* **96,** 3342–3344
6. Polymeropoulos, M. H., Lavedan, C., Leroy, E., Ide, S. E., Dehejia, A., Dutra, A., Pike, B., Root, H., Rubenstein, J., Boyer, R., Stenroos, E. S., Chandrasekharappa, S., Athanassiadou, A., Papapetropoulos, T., Johnson, W. G., Lazzarini, A. M., Duvoisin, R. C., Di Iorio, G., Golbe, L. I., and Nussbaum, R. L. (1997) *Science* **276,** 2045–2047
7. Kruger, R., Kuhn, W., Muller, T., Woitalla, D., Graeber, M., Kosel, S., Przuntek, H., Epplen, J. T., Schols, L., and Riess, O. (1998) *Nat. Genet.* **18,** 106–108
8. Zarranz, J. J., Alegre, J., Gomez-Esteban, J. C., Lezcano, E., Ros, R., Ampuero, I., Vidal, L., Hoenicka, J., Rodriguez, O., Atares, B., Llorens, V., Gomez Tortosa, E., del Ser, T., Munoz, D. G., and de Yebenes, J. G. (2004) *Ann. Neurol.* **55,** 164–173
9. Hashimoto, M., Rockenstein, E., Mante, M., Mallory, M., and Masliah, E. (2001) *Neuron* **32,** 213–223
10. Park, J. Y., and Lansbury, P. T., Jr. (2003) *Biochemistry* **42,** 3696–3700
11. Ji, H., Liu, Y. E., Jia, T., Wang, M., Liu, J., Xiao, G., Joseph, B. K., Rosen, C., and Shi, Y. E. (1997) *Cancer Res.* **57,** 759–764
12. Lavedan, C., Leroy, E., Dehejia, A., Buchholtz, S., Dutra, A., Nussbaum, R. L., and Polymeropoulos, M. H. (1998) *Hum. Genet.* **103,** 106–112
13. Zhao, W., Liu, H., Liu, W., Wu, Y., Chen, W., Jiang, B., Zhou, Y., Xue, R., Luo, C., Wang, L., Jiang, J. D., and Liu, J. (2006) *Int. J. Oncol.* **28,** 1081–1088
14. Li, Z., Sclabas, G. M., Peng, B., Hess, K. R., Abbruzzese, J. L., Evans, D. B., and Chiao, P. J. (2004) *Cancer* **101,** 58–65
15. Iwaki, H., Kageyama, S., Isono, T., Wakabayashi, Y., Okada, Y., Yoshimura, K., Terai, A., Arai, Y., Iwamura, H., Kawakita, M., and Yoshiki, T. (2004) *Cancer Sci.* **95,** 955–961
16. Jia, T., Liu, Y. E., Liu, J., and Shi, Y. E. (1999) *Cancer Res.* **59,** 742–747
17. Liu, H., Liu, W., Wu, Y., Zhou, Y., Xue, R., Luo, C., Wang, L., Zhao, W., Jiang, J. D., and Liu, J. (2005) *Cancer Res.* **65,** 7635–7643
18. Gupta, A., Inaba, S., Wong, O. K., Fang, G., and Liu, J. (2003) *Oncogene* **22,** 7593–7599
19. Inaba, S., Li, C., Shi, Y. E., Song, D. Q., Jiang, J. D., and Liu, J. (2005) *Breast Cancer Res. Treat.* **94,** 25–35
20. Jiang, Y., Liu, Y. E., Lu, A., Gupta, A., Goldberg, I. D., Liu, J., and Shi, Y. E. (2003) *Cancer Res.* **63,** 3899–3903
21. West, A. B., Dawson, V. L., and Dawson, T. M. (2005) *Trends Neurosci.* **28,** 348–352
22. Wang, F., Denison, S., Lai, J. P., Philips, L. A., Montoya, D., Kock, N., Schule, B., Klein, C., Shridhar, V., Roberts, L. R., and Smith, D. I. (2004) *Genes Chromosomes Cancer* **40,** 85–96
23. Picchio, M. C., Martin, E. S., Cesari, R., Calin, G. A., Yendamuri, S., Kuroki, T., Pentimalli, F., Sarti, M., Yoder, K., Kaiser, L. R., Fishel, R., and Croce, C. M. (2004) *Clin. Cancer Res.* **10,** 2720–2724
24. Liu, Y., Lashuel, H. A., Choi, S., Xing, X., Case, A., Ni, J., Yeh, L. A., Cuny, G. D., Stein, R. L., and Lansbury, P. T., Jr. (2003) *Chem. Biol.* **10,** 837–846
25. Caballero, O. L., Resto, V., Patturajan, M., Meerzaman, D., Guo, M. Z., Engles, J., Yochem, R., Ratovitski, E., Sidransky, D., and Jen, J. (2002) *Oncogene* **21,** 3003–3010
26. Nagakubo, D., Taira, T., Kitaura, H., Ikeda, M., Tamai, K., Iguchi-Ariga, S. M., and Ariga, H. (1997) *Biochem. Biophys. Res. Commun.* **231,** 509–513
27. Kim, R. H., Peters, M., Jang, Y., Shi, W., Pintilie, M., Fletcher, G. C., DeLuca, C., Liepa, J., Zhou, L., Snow, B., Binari, R. C., Manoukian, A. S., Bray, M. R., Liu, F. F., Tsao, M. S., and Mak, T. W. (2005) *Cancer Cell* **7,** 263–273
28. Kawashima, M., Suzuki, S. O., Doh-ura, K., and Iwaki, T. (2000) *Acta Neuropathol. (Berl.)* **99,** 154–160
29. Fung, K. M., Rorke, L. B., Giasson, B., Lee, V. M., and Trojanowski, J. Q. (2003) *Acta Neuropathol. (Berl.)* **106,** 167–175
30. Bruening, W., Giasson, B. I., Klein-Szanto, A. J., Lee, V. M., Trojanowski, J. Q., and Godwin, A. K. (2000) *Cancer* **88,** 2154–2163
31. Hashimoto, M., Yoshimoto, M., Sisk, A., Hsu, L. J., Sundsmo, M., Kittel, A., Saitoh, T., Miller, A., and Masliah, E. (1997) *Biochem. Biophys. Res. Commun.* **237,** 611–616
32. Stefanis, L., Kholodilov, N., Rideout, H. J., Burke, R. E., and Greene, L. A. (2001) *J. Neurochem.* **76,** 1165–1176
33. Takeda, A., Hashimoto, M., Mallory, M., Sundsumo, M., Hansen, L., and Masliah, E. (2000) *Acta Neuropathol. (Berl)* **99,** 296–304
34. Takenouchi, T., Hashimoto, M., Hsu, L. J., Mackowski, B., Rockenstein, E., Mallory, M., and Masliah, E. (2001) *Mol. Cell. Neurosci.* **17,** 141–150
35. Hashimoto, M., Takenouchi, T., Rockenstein, E., and Masliah, E. (2003) *J. Neurochem.* **85,** 1468–1479
36. Tanimoto, Y., Yokozeki, M., Hiura, K., Matsumoto, K., Nakanishi, H., Matsumoto, T., Marie, P. J., and Moriyama, K. (2004) *J. Biol. Chem.* **279,** 45926–45934
37. Martin-Clemente, B., Alvarez-Castelao, B., Mayo, I., Sierra, A. B., Diaz, V., Milan, M., Farinas, I., Gomez-Isla, T., Ferrer, I., and Castano, J. G. (2004) *J. Biol. Chem.* **279,** 52984–52990
38. Nakai, M., Toshimori, K., Yoshinaga, K., Nasu, T., and Hess, R. A. (1998) *Cell Tissue Res.* **294,** 145–152
39. Wyke, S. M., and Tisdale, M. J. (2006) *Life Sci.* **78,** 2898–2910
40. Ostrerova, N., Petrucelli, L., Farrer, M., Mehta, M., Choi, P., Hardy, J., and Wolozin, B. (1999) *J. Neurosci.* **19,** 5782–5791
41. Ghee, M., Fournier, A., and Mallet, J. (2000) *J. Neurochem.* **75,** 2221–2224
42. Snyder, H., Mensah, K., Theisler, C., Lee, J., Matouschek, A., and Wolozin, B. (2003) *J. Biol. Chem.* **278,** 11753–11759
43. Lindersson, E., Beedholm, R., Hojrup, P., Moos, T., Gai, W., Hendil, K. B., and Jensen, P. H. (2004) *J. Biol. Chem.* **279,** 12924–12934
44. Rubinsztein, D. C. (2006) *Nature* **443,** 780–786
45. Garrett, I. R., Chen, D., Gutierrez, G., Zhao, M., Escobedo, A., Rossini, G., Harris, S. E., Gallwitz, W., Kim, K. B., Hu, S., Crews, C. M., and Mundy, G. R. (2003) *J. Clin. Investig.* **111,** 1771–1782
46. Obin, M., Mesco, E., Gong, X., Haas, A. L., Joseph, J., and Taylor, A. (1999) *J. Biol. Chem.* **274,** 11789–11795
47. Giasson, B. I., Bruening, W., Durham, H. D., and Mushynski, W. E. (1999) *J. Neurochem.* **72,** 1081–1087
48. Pasquini, L. A., Paez, P. M., Moreno, M. A., Pasquini, J. M., and Soto, E. F. (2003) *J. Neurosci.* **23,** 4635–4644
49. Snyder, H., Mensah, K., Hsu, C., Hashimoto, M., Surgucheva, I. G., Festoff, B., Surguchov, A., Masliah, E., Matouschek, A., and Wolozin, B. (2005) *J. Biol. Chem.* **280,** 7562–7569
50. Seo, J. H., Rah, J. C., Choi, S. H., Shin, J. K., Min, K., Kim, H. S., Park, C. H., Kim, S., Kim, E. M., Lee, S. H., Lee, S., Suh, S. W., and Suh, Y. H. (2002) *FASEB J.* **16,** 1826–1828
51. Bose, S., Stratford, F. L., Broadfoot, K. I., Mason, G. G., and Rivett, A. J. (2004) *Biochem. J.* **378,** 177–184
52. Webb, J. L., Ravikumar, B., Atkins, J., Skepper, J. N., and Rubinsztein, D. C. (2003) *J. Biol. Chem.* **278,** 25009–25013
53. Cuervo, A. M., Stefanis, L., Fredenburg, R., Lansbury, P. T., and Sulzer, D. (2004) *Science* **305,** 1292–1295
54. Mizushima, N. (2005) *Cell Death Differ.* **12,** Suppl. 2, 1535–1541
55. Chen, Q., Thorpe, J., and Keller, J. N. (2005) *J. Biol. Chem.* **280,** 30009–30017
56. Tanaka, Y., Engelender, S., Igarashi, S., Rao, R. K., Wanner, T., Tanzi, R. E., Sawa, A., V. L. D., Dawson, T. M., and Ross, C. A. (2001) *Hum. Mol. Genet.* **10,** 919–926
57. Lee, S. S., Kim, Y. M., Junn, E., Lee, G., Park, K. H., Tanaka, M., Ronchetti, R. D., Quezado, M. M., and Mouradian, M. M. (2003) *Neurobiol. Aging* **24,** 687–696
58. Iwata, A., Maruyama, M., Kanazawa, I., and Nukina, N. (2001) *J. Biol. Chem.* **276,** 45320–45329
59. Abou-Sleiman, P. M., Muqit, M. M., and Wood, N. W. (2006) *Nat. Rev. Neurosci.* **7,** 207–219

ELSEVIER

Bone 40 (2007) 997–1005

BONE

www.elsevier.com/locate/bone

Association of a single-nucleotide variation (A1330V) in the low-density lipoprotein receptor-related protein 5 gene (*LRP5*) with bone mineral density in adult Japanese women

Yoichi Ezura [a,*], Toshiaki Nakajima [a], Tomohiko Urano [b], Yoshihiro Sudo [a], Mitsuko Kajita [a], Hideyo Yoshida [c], Takao Suzuki [c], Takayuki Hosoi [d], Satoshi Inoue [b], Masataka Shiraki [e], Mitsuru Emi [a]

[a] *Department of Molecular Biology, Institute of Gerontology, Nippon Medical School, 1-396, Kosugi-cho, Nakahara-ku, Kawasaki 211-8533, Japan*
[b] *Department Geriatric Medicine, Faculty of Medicine, University of Tokyo, Tokyo, Japan*
[c] *Department Epidemiology, Tokyo Metropolitan Institute of Gerontology, Tokyo, Japan*
[d] *Department Internal Medicine, Tokyo Metropolitan Geriatric Hospital, Tokyo, Japan*
[e] *Research Institute and Practice for Involutional Diseases, Nagano, Japan*

Received 20 October 2004; revised 29 May 2005; accepted 13 June 2005
Available online 15 February 2007

Abstract

Low-density lipoprotein receptor-related protein 5 (LRP5), a co-receptor of Wnt signaling, is an important regulator of bone development and maintenance. Recently we identified correlation between an intronic single-nucleotide polymorphism (SNP) in the *LRP5* gene and vertebral bone mineral density (BMD), indicating that a genetic ground exists at this locus for determination of BMD. In the study reported here, we searched for nucleotide variation(s) that might confer susceptibility to osteoporosis among an extended panel of 387 healthy subjects recruited from the same hospital (Group-A), as well as among 384 subjects from the general population in eastern Japan (Group-B). We basically focused on two potentially functional variations, Q89R (c.266A > G) and A1330V (c.3989C > T), whose functional effects by the amino-acid changes were estimated by the SIFT software program; it predicted the 1330 V allele as deleterious ("intolerant") although the minor allele of Q89R was questionable. By analyzing associations between the variant alleles and the BMD, reproducible association of the minor variant of A1330V to lower adjusted BMD levels was detected; i.e., In Group-A subjects 1330-V significantly associated with the spinal BMD *Z*-score ($P = 0.034$), and in Group-B it associated with low radial BMD ($P = 0.019$). From haplotype and linkage disequilibrium (LD) analysis for 29 SNPs, we detected two separate LD blocks within the entire 137-kb *LRP5* locus, basically consistent with a previous report on Caucasians. One of the second block haplotype significantly associated with adjusted BMD ($r = 0.15$, $P = 0.004$). Possible combined effect of Q89R and A1330V belonging to different LD blocks was denied by multiple regression analyses. Our results indicate that genetic variations in *LRP5* are important factors affecting BMD in adult women and that 1330 V may contribute to osteoporosis susceptibility, at least in Japanese.

Keywords: Single-nucleotide polymorphism; LRP5; Low-density lipoprotein receptor-related protein; Bone mineral density; Association study; Quantitative trait

Introduction

Osteoporosis is a common, multi-factorial disease characterized by reduced bone mass, microarchitectual deterioration of bone tissue, and increased risk of fragility fractures. Achievement of high peak bone mass before maturation, as well as avoidance of postmenopausal bone loss, is important for prevention of osteoporosis [1]. Since complicated processes during periods of development, maturation, and aging are regulated through multiple endocrine and local systems, many aspects of the mechanisms affecting control of bone mass remain to be clarified.

Wnt signaling is likely to be one of the most important systems involved in regulating developmental and homeostatic control of the skeletal system [2–4]. Low-density lipoprotein receptor-related protein 5 (LRP5) is a co-receptor for Wnt [5,6],

* Corresponding author. Present address: 2-3-10 Kanda-Surugadai, Chiyoda-ku, Tokyo, Tokyo Medical and Dental University, Medical Research Institute, Department of Molecular Pharmacology. Fax: +81 3 5280 8067.
E-mail address: ezura.mph@mri.tmd.ac.jp (Y. Ezura).

8756-3282/$ - see front matter © 2007 Published by Elsevier Inc.
doi:10.1016/j.bone.2005.06.025

and by studies on osteoporosis pseudoglioma syndrome (OPPG) family, causative mutations were identified in the *LRP5* gene [7,8]. On the other hand, certain mutations in *LRP5* cause an inherited trait of high bone mass in some families [9,10], and autosomal-dominant osteopetrosis in others [11]. These observations strongly suggest an important general role of LRP5 in acquisition and/or maintenance bone mass.

Genes responsible for monogenic inherited diseases sometimes also play roles in the phenotypic manifestations of common diseases [12–14], and thus are first-choice candidates for testing associations. Previously we suggested a possible contribution of LRP5 in determination of BMD, after detecting an intronic nucleotide variation of the *LRP5* gene (IVS17-1677C > A) associated with age-adjusted values of spinal BMD (*Z*-score) in a set of adult Japanese women. Although no definitive responsible variation(s) were established at that time [15], three other groups subsequently reported association of different missense nucleotide variations in *LRP5* with bone mineral density among Asian populations (Korean and Japanese; Q89R and A1330V [16,17]) and in Caucasians (V667M [18]). Although the significance levels and the suggested responsible variations were different, the reports were consistent in implicating the *LRP5* locus.

To examine in more detail the possibly responsible variation(s) of that gene in terms of BMD, we investigated multiple genetic variations within the *LRP5* locus in two independently recruited subject groups, comprising a total of 771 adult women in Japan. We constructed haplotypes, analyzed linkage disequilibrium (LD), and searched for mutations in these subjects.

Materials and methods

Subjects

The 308 subjects recruited for the previous report [15] were from an outpatient clinic in Nagano prefecture (Research Institute and Practice for Involutional Diseases). Although BMD levels distributed in a wide range without skewness, these subjects were not from a population-based panel, and thus adjustment by multiple regression was not applicable. However instead, quantitative association analysis was possible using spinal BMD *Z*-scores, and we detected significant association with an intronic variant of *LRP5*. To verify that association, extended panel of 387 adult female was recruited from the same clinic (Group-A); these are basically healthy individuals who visited the same clinic up to December 2003. Mean ages and body mass indices (BMI) with standard deviations (SD) were 64.6 ± 10.8 (range 25–89) years and 22.2 ± 2.9 (range 14.3–32.9) kg/m^2, respectively. The BMD of lumbar vertebral bodies (from L2 to L4; expressed in g/cm^2) was measured in each participant by DXA using DPX-L (GE Medical Systems Lunar Corporation, Madison WI). Coefficients of variation (CV) for the anteroposterior view of the lumbar BMD was 0.5 ± 0.5% (CV ± SD) as described [40]. *Z*-scores were calculated using installed software (Lunar DPX-L) on the basis of data from 20,000 Japanese women [19]. Eight of the subjects had remarkably high BMD (*Z*-scores > 3.0),

Table 1
Summary of LRP5 polymorphisms analyzed among 384 adult women in the general Japanese population

No.	SNP name	nt.	cSNP characteristics †	dbSNP-ID ‡	Allele frequency (%-Heterozygosity)	*n* §	Distance (bp) *	Genotyping method
1	IVS1 + 4689C > G	G/C		rs312014	0.53:0.47 (45)	378	9469	TaqMan
2	IVS1 + 14158G > A	G/A		rs312024	0.44:0.56 (46)	383	310	Invader
3	IVS1 + 14468T > C	T/C		rs634008	0.26:0.74 (41)	367	7259	Sd-PCR
4	IVS1-13315A > G	G/A		rs606989	0.91:0.09 (16)	378	9089	TaqMan
5	IVS1-4226T/C	T/C		rs74744	0.09:0.91 (18)	384	3832	Invader
6	IVS1-394A/G	A/G		rs312782	0.09:0.91 (17)	369	567	Sd-PCR
7	Q89R	A/G	(c.266A > G)	–	0.93:0.07 (13)	383	3075	Invader
8	IVS2 + 2852T > C	T/C		rs312783	0.09:0.91 (18)	381	197	Sd-PCR
9	IVS2 + 3049T > C	T/C		rs312784	0.11:0.89 (21)	375	3535	Sd-PCR
10	IVS2 + 2823T > G	T/G		rs312788	0.09:0.91 (18)	384	9317	Invader
11	IVS4 + 201G > A	A/G		rs178352	0.91:0.09 (18)	377	21,779	TaqMan
12	IVS5-393C > T	C/T		rs3781592	0.06:0.94 (11)	381	5761	Sd-PCR
13	IVS7 + 1632G > A	G/A		rs3781590	0.09:0.91 (16)	374	11,224	Invader
14	IVS7-575T > C	T/C		rs685095	0.30:0.70 (40)	382	7134	Sd-PCR
15	c.2220C > T	C/T	Silent	rs2306862	0.26:0.74 (36)	372	218	Sd-PCR
16	IVS10 + 120T > C			rs667126	0.30:0.70 (40)	384	907	Invader
17	IVS10-269C > T	C/T		rs583545	0.33:0.67 (45)	370	33	Sd-PCR
18	IVS10-236A > G	A/G		rs23691	0.34:0.66 (42)	381	498	Invader
19	IVS11 + 78G > A	G/A		rs689179	0.30:0.70 (41)	378	13,524	Sd-PCR
20	c.3357A > G	A/G	Silent	rs556442	0.42:0.58 (51)	373	6662	Sd-PCR
21	IVS17-1718G/del	G/del		rs3837372	0.39:0.61 (46)	383	41	Invader
22	IVS17-1677C > A	C/A		rs3781586	0.28:0.72 (41)	375	941	Sd-PCR
23	IVS17-376G > A	G/A		rs3781585	0.05:0.95 (10)	379	110	Sd-PCR
24	IVS17-626G > A	G/A		rs3781584	0.05:0.95 (10)	383	101	Invader
25	IVS17-525C > T	C/T		rs3781583	0.05:0.95 (10)	384	750	Invader
26	A1330V	C/T	(c.3989C > T)	rs3736228	0.26:0.71 (40)	384	1285	Invader
27	IVS18 + 1274A > G	A/G		rs638076	0.39:0.61 (44)	377	2998	Sd-PCR
28	IVS19-336T > C	T/C		rs901823	0.36:0.64 (44)	370	4140	Sd-PCR
29	IVS21 + 2334T > C	T/C		rs3781579	0.19:0.83 (28)	375	–	Sd-PCR

* Number of nucleotides to the next SNP (bp).
† Nucleotide positions in the coding sequence are indicated for missense cSNPs.
‡ IDs are from dbSNP of NCBI (http://www.ncbi.nlm.nih.gov/SNP/).
§ Number of genotyped subjects.

Table 2
Association analysis of adjusted BMD in Groups-A and -B

SNP	Genotype	Group-A (n = 387) (spinal BMD Z-score)		P value[a]	Group-B (n = 384) (radial-adjusted BMD)		P value[a]
		Mean ± SD	n		Mean ± SD	n	
Q89R	Q	−0.15 ± 1.50	332	0.85	0.401 ± 0.055	333	0.052
	QR	−0.14 ± 1.54	35		0.387 ± 0.049	48	
	R	−0.57 ± 1.10	3		0.360 ± 0.059	2	
A1330V	A	−0.04 ± 1.61	178	0.034 *	0.405 ± 0.053	195	0.019 *
	AV	−0.35 ± 1.38	174		0.395 ± 0.059	155	
	VV	−0.47 ± 1.47	35		0.385 ± 0.041	34	
MC17-1677C > A (before expansion)	CC	−0.01 ± 1.42	166	0.005 **	0.405 ± 0.053	194	0.055
	CA	−0.35 ± 1.44	118		0.395 ± 0.059	152	
	A	−0.78 ± 1.36	24		0.390 ± 0.040	29	

±Data were from the previous study before subject expansion.
[a] P values were calculated for the linear regression.
* $P < 0.05$.
** $P < 0.01$.

and four had remarkably low BMD (Z-scores < −3.0). For distribution analysis, we selected 91 subjects with Z-scores > +1.0 and 139 with Z-scores < −1.0. Among those women, the Z-score was greater than 2.0 in 33 and smaller than −2.0 in 34 of them. Biochemical markers of bone turnover including serum intact osteocalcin, urinary pyridinoline, and deoxypyridinoline were measured in most of the 387 subjects ascertained from the Institute; each had given informed consent prior to the study.

DNA samples for a population-based analysis were obtained from peripheral blood of 384 adult Japanese women [20,21]. In this group (Group-B), mean ages and body mass indices (BMI) with standard deviations (SD) were 58.4 ± 8.6 (range 32–69) years and 23.7 ± 3.61 (range 14.7–38.5) kg/m^2, respectively. The BMD of radial bone (expressed in g/cm^2) of each participant was measured by dual energy X-ray absorptiometry (DXA) using DTX-200 (Osteometer Meditech Inc., Hawthorne, CA, USA) and was normalized for differences in age, height, and weight by multiple linear regression analysis [21]. Forearm BMD in the distal radius was measured according to the Guidelines for Osteoporosis Screening in a health check-up program in Japan [22]; the instruments (DTX-200) were calibrated at every measurement, and the coefficients of variation were kept within the 1.0 ± 0.5% (CV ± SD). No participant had medical complications or was undergoing treatment for conditions known to affect bone metabolism [21]. All were non-related volunteers, and written informed consent was obtained from each of them. The ethical committee of the Institutional Review Board approved the entire project.

Mutation search, SNP selection, and genotyping

Mutation analysis of all 23 exons and flanking regions was carried out in DNA from the 12 subjects with the highest (>3.0, n = 8) and lowest (<−3.0, n = 4) Z-scores by direct sequencing of PCR products in the ABI Prism 377 DNA system (Applied Biosystems).

As potentially functional SNPs, two previously reported missense coding-SNPs, A1330V (c.3989C > T) and Q89R (c.266A > G), were selected for testing association of BMD levels, but a third, V667M, was eliminated because it was undetectable among our subjects (Table 1). Another intronic variation previously reported to associate with low BMD also was tested for association. For LD analysis, we first tested more than 40 variations within the *LRP5* locus, including all 38 polymorphic variations archived in the JSNP-database (http://snp.ims.u-tokyo.ac.jp/index.html), dbSNP, and from the literature [11,23]. However, since some of the variations showed minor allele frequencies of <0.05 among our Group-B 384 subjects, we chose to use only 29 SNPs for LD analysis.

Genotypes for these 29 selected SNPs were determined either by the Sd-PCR method [20], Invader assay (Third Wave Technologies, Madison, WI) [24], or TaqMan Assay (Applied Biosystems). The Sd-PCR method was used for 16 SNPs, according to a protocol described previously [20]. In brief, the Sd-PCR reaction was carried out using two allele-specific primers (AS-primers) and one reverse primer in a standard reaction mixture containing fluorescence-labeled dCTP. Discrimination of alleles, on the basis of by five-base differences between the AS-primers, was achieved using an ABI Prism 377 DNA system [21]. The Invader assay was applied for 10 other SNPs, according to the manufacturer's protocol. In brief, 1 μl of the diluted PCR product (1:333 in distilled water) of the region flanking each SNP was used as template in a 6-μl reaction mixture in 384-well plates, and fluorescent signals for FAM and Redmond Red were detected by a plate-reader after standard 1-h incubation [25]. The other three SNPs were genotyped by TaqMan Assay according to the manufacturer's protocol.

Table 3
Physical and clinical characteristics of the subjects in Group-A (healthy subjects from a clinic)

Group-A subjects (n = 387)	A1330V			P value *
	AA	AV	VV	
Number	178	174	35	–
Age (Years)	65.6 ± 10.1 (41–86)	64.1 ± 10.4 (33–89)	59.3 ± 15.0 (25–87)	0.012
Weight (kg)	51.1 ± 7.9 (34–74)	50.0 ± 7.9 (33–76)	50.2 ± 8.1 (34–70)	NS
BMI (kg/m^2)	22.5 ± 3.0 (16.4–32.9)	21.9 ± 2.7 (14.3–31.8)	21.9 ± 3.2 (15.3–29.5)	NS
Height (cm)	150.8 ± 6.2 (135–167)	150.8 ± 6.7 (134–172)	151.1 ± 5.4 (140–162)	NS
Spine BMD (g/cm^2)	0.914 ± 0.215 (0.387–1.732)	0.878 ± 0.188 (0.400–1.506)	0.898 ± 0.196 (0.518–1.310)	NS
BMD Z-score	−0.03 ± 1.62 (−3.1–7.1)	−0.35 ± 1.38 (−3.5–5.3)	−0.45 ± 1.47 (−2.9–3.1)	0.034
Intact-OC (ng/ml)[†]	7.18 ± 3.16 (n = 117)	8.40 ± 3.82 (n = 118)	8.87 ± 3.81 (n = 18)	0.004
Pyridinoline (pmol/μmol crea.)	34.2 ± 11.1 (n = 138)	33.6 ± 11.2 (n = 133)	34.5 ± 11.4 (n = 20)	NS
Deoxypyridinoline (pmol/μmol crea.)	7.20 ± 2.50 (n = 139)	7.29 ± 2.42 (n = 133)	7.85 ± 3.01 (n = 20)	NS

* P values are calculated for regression analysis with ANOVA F-test.
[†] Serum intact osteocalcin level.